Chapter 4

Facile synthesis of fluorescent Carbon Quantum dots from Palm Shell Powder and graphene quantum dots from Diethylenetriamine Pentaacetic acid for sensing of Nitrophenols

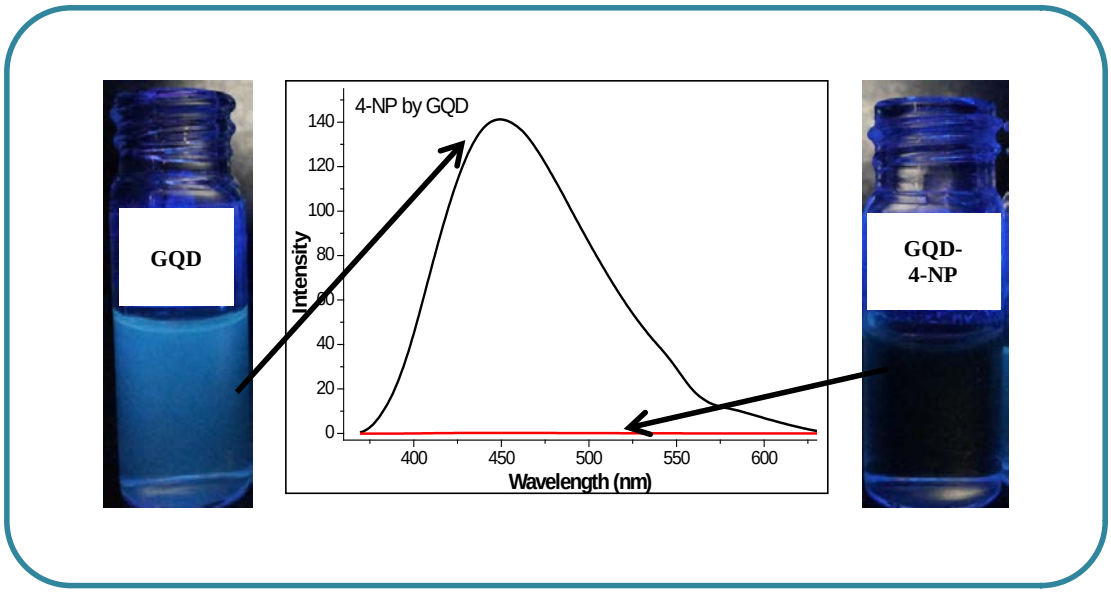

4.1 Introduction

Carbon dots (CDs) are newly emerging carbon nanomaterials, which mainly include carbon nps of size less than 10 nm, also called carbon quantum dots, CQDs (Sun et al., 2006). They exhibit unique optical properties such as fluorescence, chemiluminescence and electrochemiluminescence due to their quantum confinement and edge effects. Furthermore, they present many advantages including low toxicity, low cost, robust chemical and optical inertness over semiconductor based quantum dots (Dong et al., 2015). CDs have great potential applications in various fields, including bio-imaging, cell-imaging, sensing, photovoltaic devices and catalysis (Baker and Baker, 2010; Liu et al., 2012; Lu et al., 2012; Shen et al., 2012; Zhang Z. et al., 2012).

Another fascinating new addition into the carbon family is graphene (Geim and Novoselov, 2007), the one-atom thick sheets of carbon. Graphene is a two-dimensional (2-D) sheet of sp^2 hybridized carbon atoms arranged in a honeycomb shaped lattice with a very high surface area (~2630 m^2/g), exposing a significant fraction of surface atoms to analytes (Yu J. et al., 2015). Graphene is a semiconductor with a zero band-gap. It exhibits charge carrier mobilities exceeding 15,000–20,000 cm^2/Vs even at room temperature due to ambipolar electric field effect. This makes the electronic properties of graphene sensitive to both electron-donating and electron-withdrawing molecules. In addition, graphene exhibits superior mechanical and thermal properties, optical transparency (97.7%) and flexibility. These physical, chemical and electrical properties make graphene an attractive candidate for the fabrication of label-free electrochemical biosensors with high sensitivity (Huang et al., 2011; Ohno et al., 2010).

Graphene quantum dots (GQDs) are graphene layers smaller than 100 nm (Li Q. et al., 2012). Such nanomaterials have unusual optical and electronic properties partly arising from their quantum confinement and zigzag edge effects (Bao et al., 2011; Jin et al., 2013; Yan et al., 2013; Zheng et al., 2011). Other useful properties include: chemical inertness, strong fluorescence, high photo-stability, and low toxicity (Güttinger et al., 2012; Li J. et al., 2012; Shen et al., 2012; Zhu et al., 2012).

Till date, many simple and efficient methods have been proposed to synthesize different types of CDs and GQDs. The methods can be generally classified as “bottom-up” and “top-down”. The “bottom-up” strategies (Essig et al., 2010; Liu et

al., 2011) involve carbonizing some precursors through hydrothermal (Dong et al., 2013),thermal (Dong et al., 2012b), microwave (Zhu et al., 2009), acid oxidation (Peng and Travas-Sejdic, 2009), electrochemical or sonication treatments (Li H. et al., 2011). Usually, these "bottom-up" strategies provide advantages such as precise control over the morphology and the size distribution of the product (Liu et al., 2011; Yan et al., 2010) or convenience for surface-passivation or heteroatom doping to prepare high yield luminescent materials (Dong et al., 2013).

The top-down techniques which involve cutting down the size by different techniques may have an advantage in producing the nanomaterials on a large scale (Li H. et al., 2011; Pan et al., 2010; Peng et al., 2012). During the preparation process, the choice of various precursors results in different characteristics for the obtained carbon and GQDs.

"Top-down" techniques for CQDs involve cutting some big-size carbon sources such as graphite (Li et al., 2013; Lu et al., 2009; Zheng et al., 2009), activated carbon (Dong et al., 2010; Qiao et al., 2010), graphene or GO (Lin and Zhang, 2012; Pan et al., 2010; Zhu et al., 2012) carbon nanotubes (Lin and Zhang, 2012; Zhuo et al., 2012), carbon fibres (Peng et al., 2012), carbon black (Dong et al., 2012), candle soot (Liu et al., 2007), sugarcane bagasse pulp carbon (Thambiraj and Shankaran, 2016) by chemical oxidation (Dong et al., 2012; Peng et al., 2012), electrochemical oxidation (Zhou et al., 2007), hydrothermal (or solvothermal) treatment, (Pan et al., 2010; Shen et al., 2011; Zhu et al., 2011), electrothermal lithography (Ponomarenko et al., 2008), proton ablation and laser ablation (Sun et al., 2006) as well as preparations on solid supports (Lin et al., 2014; Zong et al., 2011).

The "bottom-up method" is often preferred for CQDs, because it is relatively easy to perform; it produces high quantum yields, and it offers precise control over the morphology and size of the quantum dots. However, these ‘‘bottom-up’’ methods are time consuming and include the need to optimize the hydrothermal treatment, temperature control and object selection (Lin et al., 2015). However, most reported precursors used in both "bottom-up" and "top-down" methods are either too expensive or difficult to obtain and are not suitable for mass production.

Recently preparation of CQDs using nontoxic solvents and economical green materials has gained prominence in a green synthetic strategy. The strategies adapted include sugarcane stalk and sodium hydroxide (Du et al., 2014), *Carica papaya* juice

and dichloromethane (Kasibabu et al., 2015), Neem gum and sodium hydroxide (Phadke et al., 2015), Mannose and ammonium citrate (Weng et al., 2015), Trapabispinosa peel (Mewada et al., 2013), Coffee grounds and hydrazine hydrate (Wang et al., 2016), Apple juice (Mehta et al., 2015), Glucose and H_2O (Li Y. et al., 2011), Anthracite and H_2O (Hu et al., 2016), Orange juice and ethylenediamine (Singh K. et al., 2014), Chicken egg and H_2O (Wang et al., 2012), Gelatin and H_2O (Liang et al., 2013), Chitosan (Yang et al., 2012), Diesel engine soot (Tripathi et al., 2014), Glucosamine and H_2O (Liu et al., 2015), Ascorbic acid and copper acetate (Jia et al., 2012), Wheat straw and milli-Q water (Yuan et al., 2015), Banana juice (De and Karak, 2013), *Saccharum officinarum* juice (Mehta et al., 2014), Soya-nuggets (Dubey et al., 2015), Cucumber/Pineapple waste (Himaja et al., 2014), *Jinhua bergamot* (Yu J. et al., 2015), Candle soot (Liu et al., 2007) and sugarcane bagasse pulp carbon (Thambiraj and Shankaran, 2016). Graphene is prepared from graphite which requires the use of a large amount of acid, oxidising agents and harsh conditions (Na et al., 2015).

The top-down methods for GQDs which refer to cutting of larger graphene sheets into nanosized ones by using physical or chemical approaches, are usually not very satisfactory due to complex process, severe conditions, expensive starting materials and low product yield (Lu et al., 2011; Shen et al., 2011).

A simple green “bottom-up” method for the synthesis of GQDs. involves the usage of a green and natural citric acid as the precursor (Roushani et al., 2015).

However, Nitrogen-doped graphene quantum dots (NGQDs) have received significant attention because doping chemically-bonded N atoms tunes their chemical reactivity and electronic properties (Qu et al., 2010). By taking advantages of their unique chemical and optical properties, N-GQDs have been widely employed in various fields such as fuel cells (Qu et al., 2010), electrocatalysis (Luo et al., 2011), biosensing (Wang Y. et al., 2010), and the detection of heavy-metal ions and small molecules (Fan et al., 2012; Zhang and Chen, 2014). The currently, available synthesis approaches employed to fabricate N-GQDs include electrochemical (Li Y. et al., 2012), organic-synthesis (Li L.-L. et al., 2012), and hydrothermal methods (Hu et al., 2013). Although several approaches have been identified to be successful for synthesizing N-GQDs for the desired possible applications, the N doping of GQDs also inevitably requires harsh reaction conditions such as bias voltages, high

temperature, high pressure, and multi-step synthesis. Moreover, these methods are complex, time consuming and expensive, which limits their widespread applications. Recently, much advancement has been made in the development of strategies to fabricate self-passivated N-GQDs through high temperature or microwave-assisted hydrothermal carbonization (Wang Y. et al., 2010; Zhang and Chen, 2014). Oxygen-rich N-doped graphene quantum dots (N-OGQDs) were prepared recently using citric acid as the carbon source and 3,4-dihydroxy-L-phenylalanine (L-DOPA) as the nitrogen source (Shi B. et al., 2015).

The attractive luminescent property of carbon dots and graphene quantum dots make them the ideal candidates to be applied as detection systems for nitrophenols. Fluorescent method has been proved to be a powerful optical technique for the trace detection of analytes due to its high sensitivity, simple instrumentation and ease of operation (Dai et al., 2014). A sensor for the analysis of trinitrophenol (TNP), has been developed using blue luminescent GQDs derived from citric acid by a pyrolysis procedure (Li et al., 2015).

Since palm shell derived carbons showed interesting properties (Chapter 3) attempts were made to prepare CQDs using palm shell as precursor.

It was also felt that if we use Diethylenetriaminepentaacetic acid (DTPA) as precursor instead of citric acid for the preparation of graphene quantum dots it would naturally provide a source of nitrogen.

Our objective was to synthesize carbon quantum dots by using palm shell derived carbon and graphene quantum dots using DTPA and investigate their ability to be used as sensors for the detection of model pollutants (Nitrophenols, chlorophenol bisphenol and pesticides like monocrotophos) under study.

PART-A

(Carbon quantum dots prepared from Palm Shell derived Carbon)

4.2 Experimental

4.2.1 Chemicals and precursor

All chemicals were of analytical reagent grade: Triflic Acid (Trifluoromethanesulfonic acid, Spectrochem, India), HCl (Hydrochloric acid, AR,Spectrochem, India), NaOH (Sodium hydroxide, LR, Spectrochem India), Phenol, 4-Chlorophenol (pCP), Monocrotophos (MnCP), 4-Nitrophenol (4-NP, $C_6H_5NO_3$), 2,4-Dinitrophenol (DNP, $C_6H_4N_2O_5$) and 2,4,6-Trinitrophenol (TNP, $C_6H_3N_3O_7$) (LR,Spectrochem, India) were used.

4.2.2 Preparation of Carbon Dots

Attempts were made to prepare CQDs from PSP derived chars. APSP was prepared in Chapter 2 by using sulfuric acid. It was felt that instead of using such acids attempts could also be made in the synthesis of CQDs by using non oxidising superacid Triflic acid treated PSP. This is the first ever attempt to the best of our knowledge.

Trifluoromethanesulfonic acid (triflic acid, TFA) is a strong non-oxidizing brønsted superacid, extensively utilized in acid catalyzed synthetic transformations (Prakash et al., 2015).

Dried PSP was treated with TFA (Sp. gr. 1.7) in ratio of 1:1.5 of PSP to TFA. The resulting mass was then digested for 10 h in an oven at 150°C. The char obtained was then washed with water followed by 2% solution of $NaHCO_3$ until effervescences ceased and then left to soak in a 2% solution of $NaHCO_3$ overnight. The Triflic acid activated palm shell char was then separated, washed with water until free of bicarbonate and dried at 105°C (TFAC).

Chemical exfoliation of APSP was done using NaOH followed by sonication while TFAC was exfoliated by just sonication. About 0.5 g of TFAC was taken in 50 mL of conductivity water and APSP was taken in 0.1 N NaOH solution. The respective suspensions were ultrasonicated for 30 min; the content was then filtered through whatmann filter paper 42, and the filtrate was then centrifuged at 10,000 rpm for 10 min to remove heavier particles. The obtained light brown color solution contained CQDs and was purified using dialysis membrane (6000-8000 Da).

The prepared CQDs exhibited a bright green colour fluorescence (Figure 4.1(a)) with the naked eye under ultraviolet radiation (λ = 365 nm).

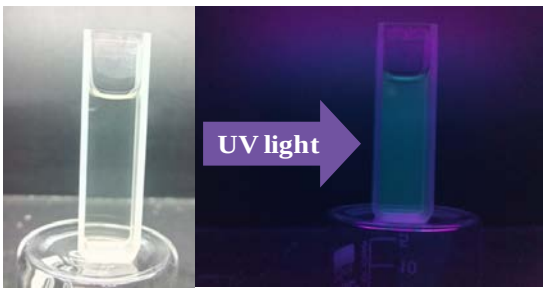

Figure 4.1(a) Fluorescence image of CQDs under UV light (365 nm)

Preliminary photoluminescence studies revealed that APSP exhibited weak fluorescence as compared to TFAC (Figure 4.1 (b)).

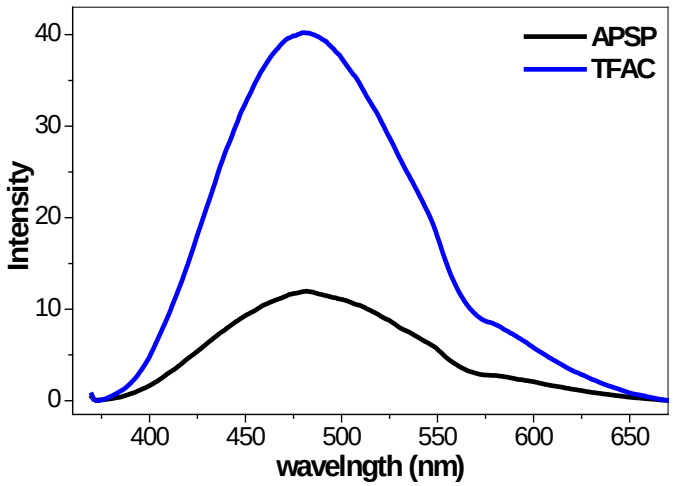

Figure 4.1(b) Fluorescence spectra of APSP and TFAC excited at 310nm

It was decided to restrict to TFAC derived CQDS for further studies. The CQDs mentioned henceforth were derived from TFAC.

The CQDs were characterized by FTIR, TEM, Raman, XPS, UV and fluorescence spectroscopic techniques.

4.2.3 Characterisation of CDs

4.2.3.1 Fourier Transform Infrared Spectroscopy (FT-IR)

FT-IR was used to determine the vibrational frequencies of the functional groups of CQDs. The spectra were collected by a Perkin-Elmer RX1 model within the wavenumber range of (400 to 4000) cm^{-1}. A CaF_2 cell was used for the measurement of FTIR of the CQDs dispersed in water. Conductivity water was taken as blank.

4.2.3.2 UV-Visible spectroscopic analysis

UV-Visible spectral measurements were carried out using a JASCO-Japan made spectrophotometer (V-630 model) working in the range 1100 nm-190 nm. Measurements were carried out in aqueous medium against water as blank.

4.2.3.3 Fluorescence measurements

Fluorescence spectra were recorded on a JASCO, FP-6300 fluorescence spectrophotometer.

4.2.3.4 Transmission Emission Microscopic (TEM) Analysis

The aqueous solutions of quantum dots samples (GQDs and CQDs) were dried on -1500 mesh copper coated TEM grid (Tecnai-12, FEI-Netherlands) for analysis. Images were taken by Single tilt holder with CCD Camera. Tecnai software was used for noise filtering.

4.2.3.5 Quantum Yield (QY) measurements

Quinine Sulphate (QS) (spectrochem India, AR grade) (1 $\mu g.mL^{-1}$) in 0.1 M H_2SO_4 (QY=54.0 %) was used as standard solution (Sahu et al., 2012). The UV-spectra and fluorescence spectra of different concentrations of QS and GQDs solutions were measured. The concentration of quantum dots (CQDs/GQDs) and QYs were selected in such a way that the absorbance from UV measurements were below 0.1 unit at 340 nm. The fluorescence quantum yield (QY) was calculated using following formula (Gu et al., 2014)

$$\emptyset_x = \emptyset_{st} \times (K_x/K_{st}) \times (\eta_x/\eta_{st})$$

Where, $\emptyset$ is fluorescence quantum yield (QY); K is slope determined from the fluorescence intensity vs. UV-Vis absorbance plot and η is refractive index. The term "st" and "x" stands for standard-QS and sample respectively. The ratio η_x/η_{st} is 1 for aqueous solution.

4.2.4 Application of CDs as sensor for Model Pollutants

The potential of CQDs for sensing of model pollutants was monitored by fluorescence measurements. In a typical experiment, 2 mL of 10% CQD solution was measured for initial fluorescence intensity. Sensing study was carried out by successive addition of analyte solution of known concentration and measuring fluorescence (310 nm excitation wavelength and 410 nm emission wavelength) under optimized experimental conditions.

4.3 Results and discussion

4.3.1Characterizations of CDs

4.3.1.1 TEM analysis

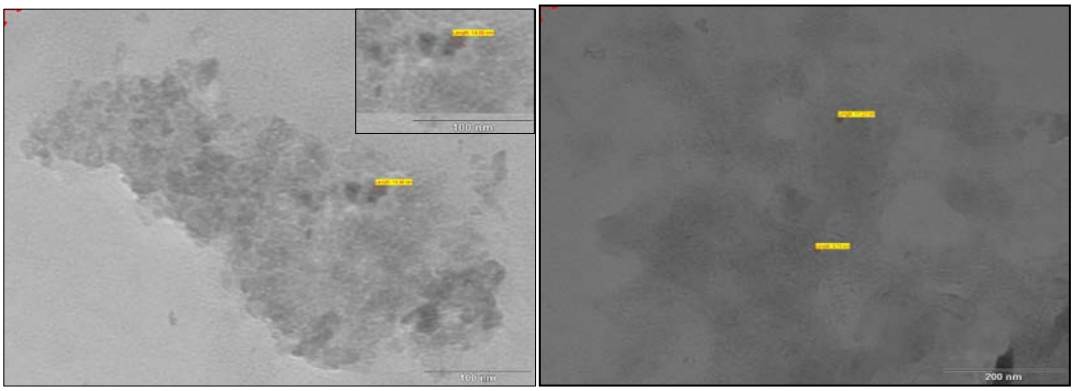

Figure 4.2 TEM image of CQDs

TEM images reveal the formation of nearly spherical particles, monodisperse with fairly uniform size in the range 4-10 nm (Figure 4.2).

4.3.1.2 FTIR analysis

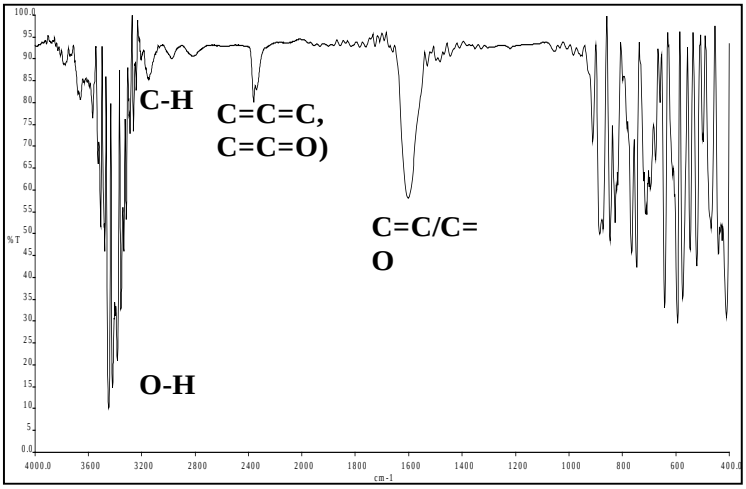

Figure 4.3 FTIR spectra of CQDs

The sharp band at ~3350 cm^{-1} observed in the FT-IR spectra of CQDs (Figure 4.3) corresponds to the stretching vibrations of O-H groups, whereas the peak centred at ~2900 cm^{-1} is typically associated with sp^3 C-H stretching vibrations. The peak centred at ~1600 cm^{-1} may be attributed to C=C and/ or C=O groups indicating that the surfaces of CQDs are surrounded by hydrophilic groups.

4.3.1.3 Raman analysis

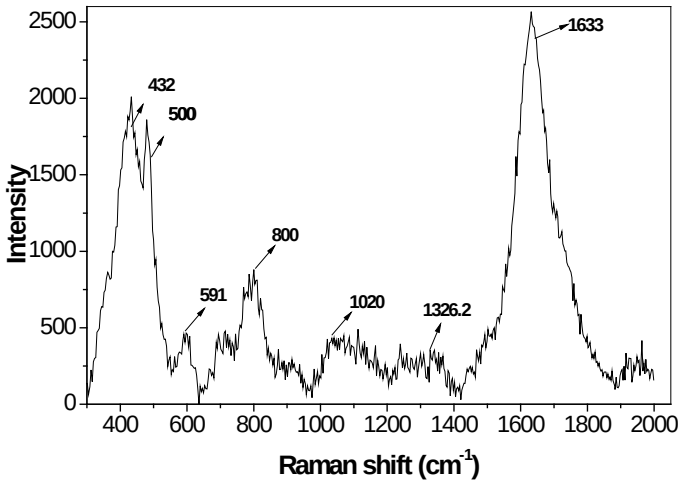

Figure 4.4 Raman spectra of CQDs

The photoluminescence background was subtracted to get a smoothened Raman spectrum, shown in Figure 4.4. The Raman spectrum of CQDs exhibits a major band at ~1633 cm^{-1}, which can be attributed to G-band (sp^2). The G band is usually assigned to a lattice vibration involving the stretching of the carbon–carbon bonds with E_{2g} symmetry that occurs within the plane of a hexagonal ring structure composed of sp^2carbon atoms. All pairs of sp^2 bonded carbon atoms are reported to generate some kind of G band. The G signal was broad suggesting different populations of carbon-carbon bonds with varying levels of strain (McDonald et al., 2013). The shift of the G band to about 33 cm^{-1} might be attributed to the small sizes of the basal graphene layers in the grains of the CQDs. The presence of a very weak D band at 1326.17 cm^{-1} suggests highly ordered graphene like structure with hexagonal aromatic rings (Ferrari and Robertson, 2004). The I_d/I_g ratio was found to be 0.2519 which also supported graphene like structure of the CQDs.

The peaks at 432 and 500 cm^{-1} are attributed to bending modes of sp linear structures and some amorphous sp^3 bonded carbon respectively (Casari et al., 2008).

4.3.1.4XPS analysis

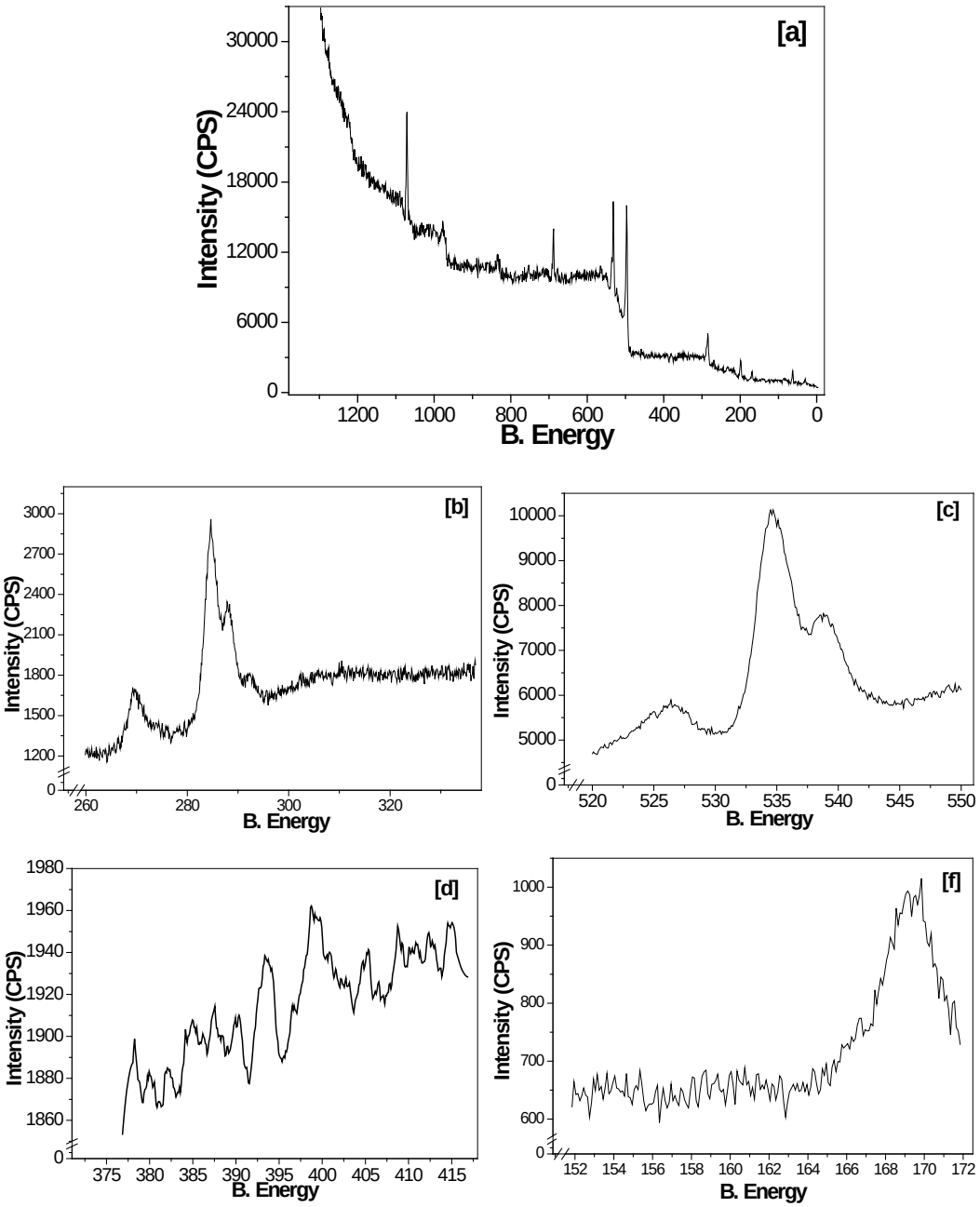

Figure 4.5 (a-e) XPS analysis spectra for CQDs

(a) Survey scans (b) C1s (c) O1s (d) N1S and (e) S2p

Figures 4.5 (a-e) depict the survey spectrum of CQDs as well as C1s, O1s, Ns and S2p spectra. The binding energies and the respective assignments are summarized in Table 4.1. The XPS data show that CQDs are mainly composed of graphitic carbon (sp^2) as well as oxygen bonded carbon with a minor amount of sulfur.

Table 4.1 XPS analysis of CQDs

CQDs					
C1s			**O1s**		
	Binding Energy (eV)	Intensity (CPS)		Binding Energy(eV)	Intensity (CPS)
C=C/ C-C	284.8	2959.662	C-O	531.9	5751.71
C-O-C	286	2246.587			
O-C=O	288.5	2255.671	C=O	533	7133.15
S2p			**N1s**		
	Binding Energy(eV)	Intensity (CPS)		Binding Energy(eV)	Intensity (CPS)
S-H	163.9	688.6074	C-NH2	399.75	1956.486

4.3.1.5 Zeta potential measurements

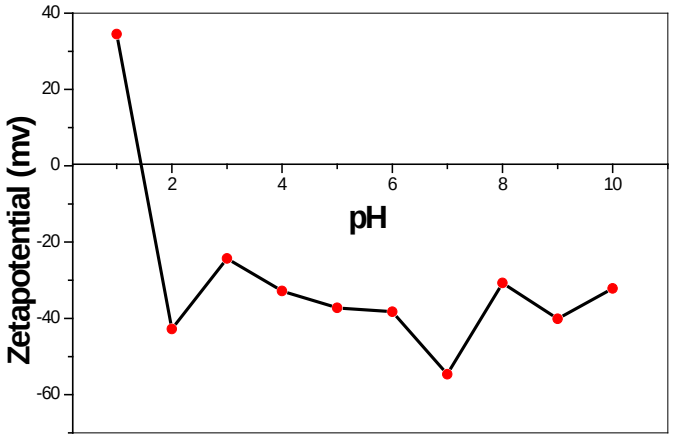

Figure 4.6 Zeta potential measurements of CQDs

The zpc value of CQDs was observed to be ~1.5 and the zeta potential was observed to be negative from pH ~1. (max.ca. -54.6 mV, at pH 7) (Figure 4.6), indicating the formation of highly negative charged surface and well dispersed stable CQDs with -C=O groups on its edges (Lin et al., 2015).

4.3.1.6 Fluorescence analysis

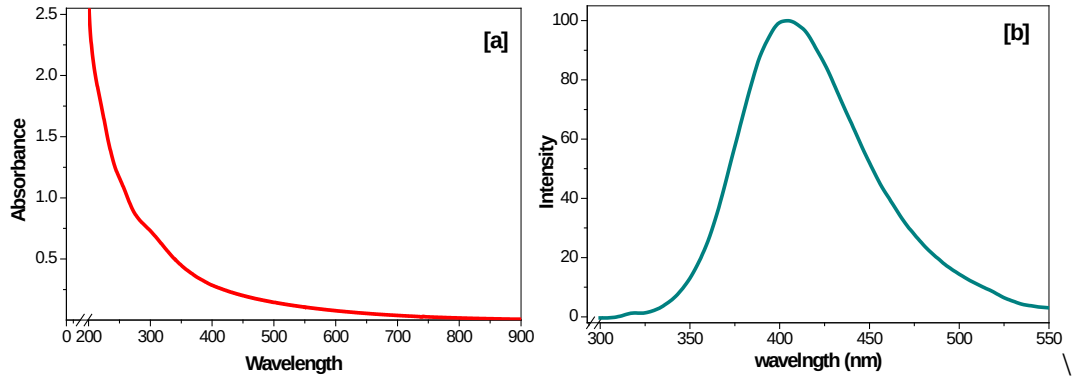

Figure 4.7 CQDs (a) Absorption spectra (b) Emission spectra

As seen in UV-visible absorption and fluorescence emission spectra in Figure 4.7 (a) and (b) respectively, the prepared CQDs exhibited a shoulder at ~278 nm, which is attributed to π-π* electron transitions. The aqueous CQD solution exhibited a fluorescence emission band at~410 nm when excited at 310 nm exhibiting a stoke shift of 100 nm. A similar photoluminescence property of CQDs has been reported by other groups (Hu et al., 2010; Peng et al., 2012). The emission property of CQDs is reported to depend on size of the CQDs, the availability of sp^2 sites, the aromatic conjugate structure, and defects of the structure.

The quantum yield was calculated to be about 0.98 % using quinine sulfate in 0.1 M sulphuric acid as the standard.

4.3.2 Optimization of fluorescence property of CQDs

4.3.2.1 Effect of excitation wavelength

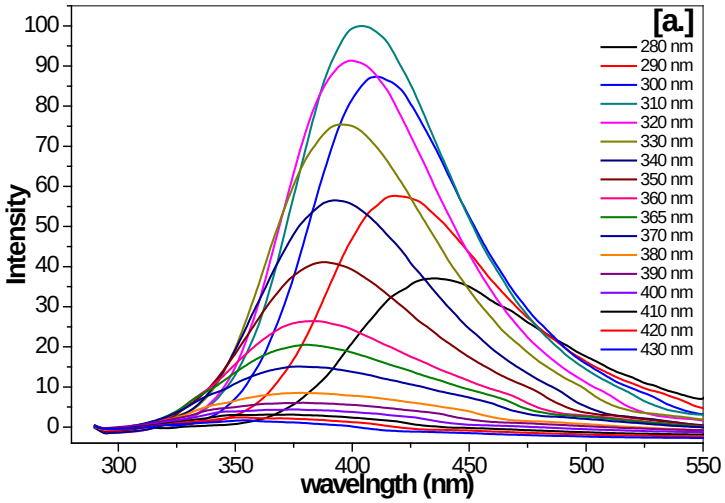

Figure 4.8 Excitation dependent fluorescence of CQDs

The CQDs were observed to exhibit excitation-dependent fluorescence behaviour (Figure 4.8), which is common for fluorescent carbon materials (Krysmann et al., 2012). The emission spectra maximum was observed to shift from 320 nm to 565 nm as the excitation wavelength varied from 280 nm to 430 nm. The maximum emission intensity was observed at ~ 410 nm (bright green emission) when excited at 310 nm. The surface state and size are reported to affect the band gap of CQDs reflecting in the fluorescence behaviour (Shang et al., 2012; F. Wang et al., 2010; Zhai et al., 2012; Zhu et al., 2013)

4.3.2.2 Effect of pH on fluorescence intensity of CQDs

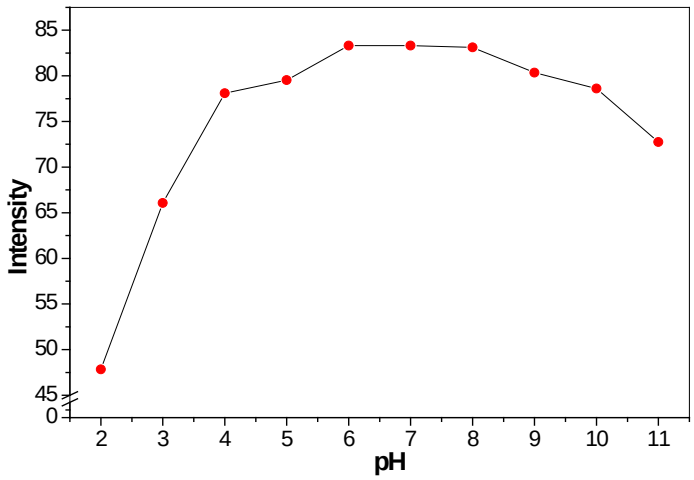

Figure 4.9 Effect of pH on fluorescence intensity of CQDs measured at 410 nm emission wavelength

A number of studies have shown that the pH of the medium strongly influences the fluorescence of CQDs (Liu et al., 2012; Wee et al., 2013). The pH of the CQDs solution was adjusted to the desired pH using 0.1 N HCl/ 0.1 N NaOH solutions. The intensity of fluorescence was observed to increase with pH increment till pH 5, was constant in the pH range 6-8 and decreased slightly with further increment in pH till pH 11 which could be attributed to protonation/ deprotonation and charge transfer involved with different type of functional groups present on the surface (Figure 4.9).The CQDs have different kinds of functional groups like C- H, C=O, C-O-C , C-OH as well as a small amount of C-NH_2, on the surface which could form a series of energy levels in surface states. These energy levels might result in formation of emissive traps (Sahu et al., 2012).

4.3.3 Sensing studies

The potential of CQDs to sense 4-NP, DNP, TNP, 4-CP, BPA and MnCP was then investigated. BPA was observed to get precipitated at all concentrations and hence was not studied further as our objective was to use aqueous solutions. It was observed from Figure 4.10 (a-f) that the fluorescence intensity of the CQDs was gradually quenched upon the addition of the analytes under study. It was found from the study that maximum fluorescence quenching was achieved by NP, DNP and TNP at concentration of 0.75 mM, 0.99 mM and 0.69 mM respectively.

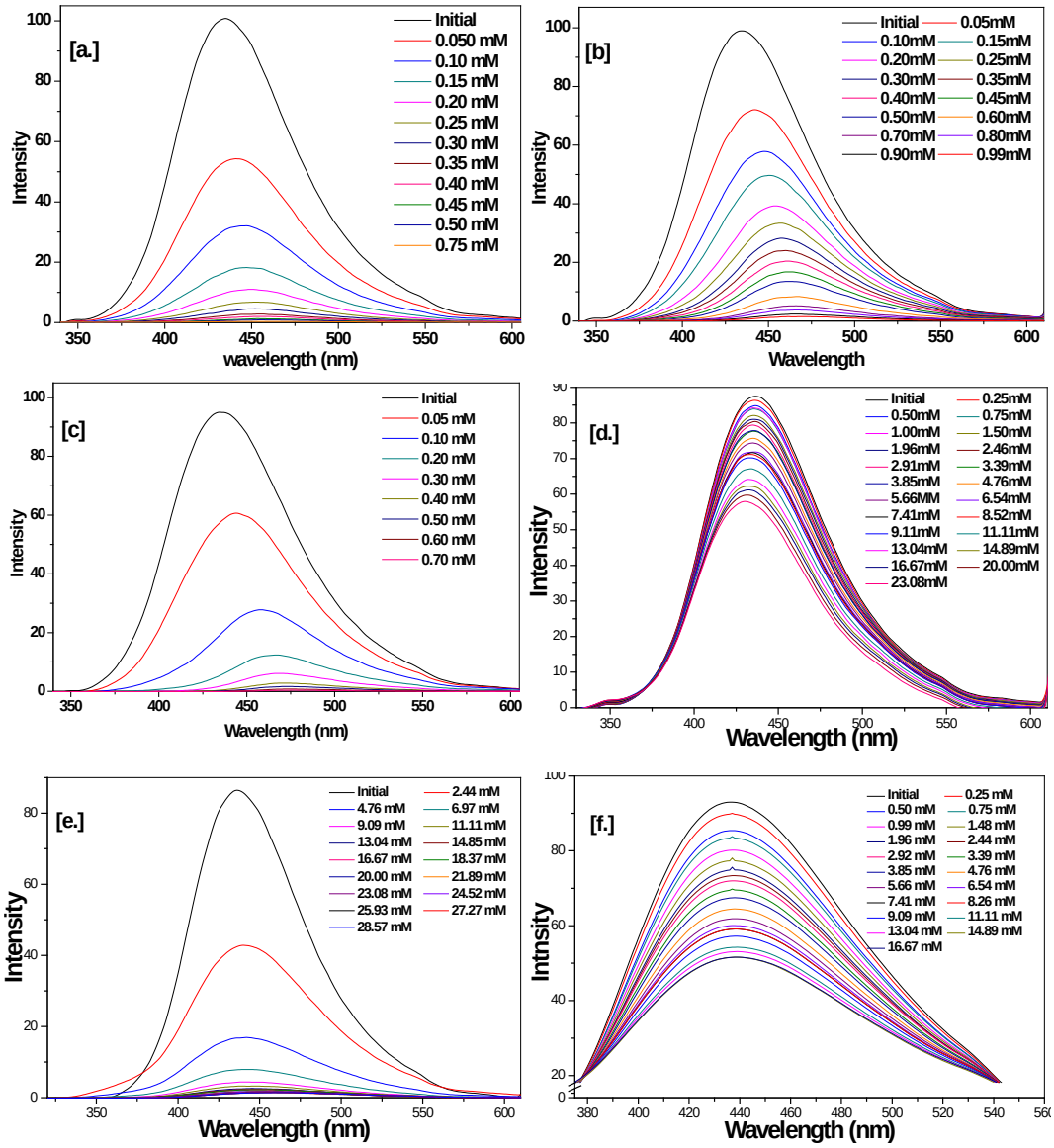

Figure 4.10 Fluorescence quenching study of CQDs with

(a) 4-NP (b) DNP (C) TNP (d) 4-CP (e) MnCP (f) Phenol

The performance of the CQDs were analysed by using the Stern-Volmer equation;

$$F_0/F = k_{SV} \cdot [Q] + 1;$$

Where F_0 is the fluorescence intensity in the absence of the quencher, F is the fluorescence intensity in the presence of the quencher, K_{SV} is the Stern-Volmer quenching constant and Q is the concentration of the quencher (Long and Winefordner, 1983). A linear graph was obtained between F_0/F vs [Q] in each case Figure 4.11(a-f). The K_{SV} values obtained from the slope indicated the order of sensitivity of the CQDs for the analytes under study (Table 4.2). The larger the K_{SV} value, the more sensitive the CQDs are to that particular analyte. Further, from the plots the detection limit for each analyte under study, defined as the concentration equivalent to $[3 \times Sd/slope]$ where sd is the standard deviation of the blank F_0, was calculated. The LOQ have been derived using formula$\text{LOQ} = [10 \times Sd/slope]$.

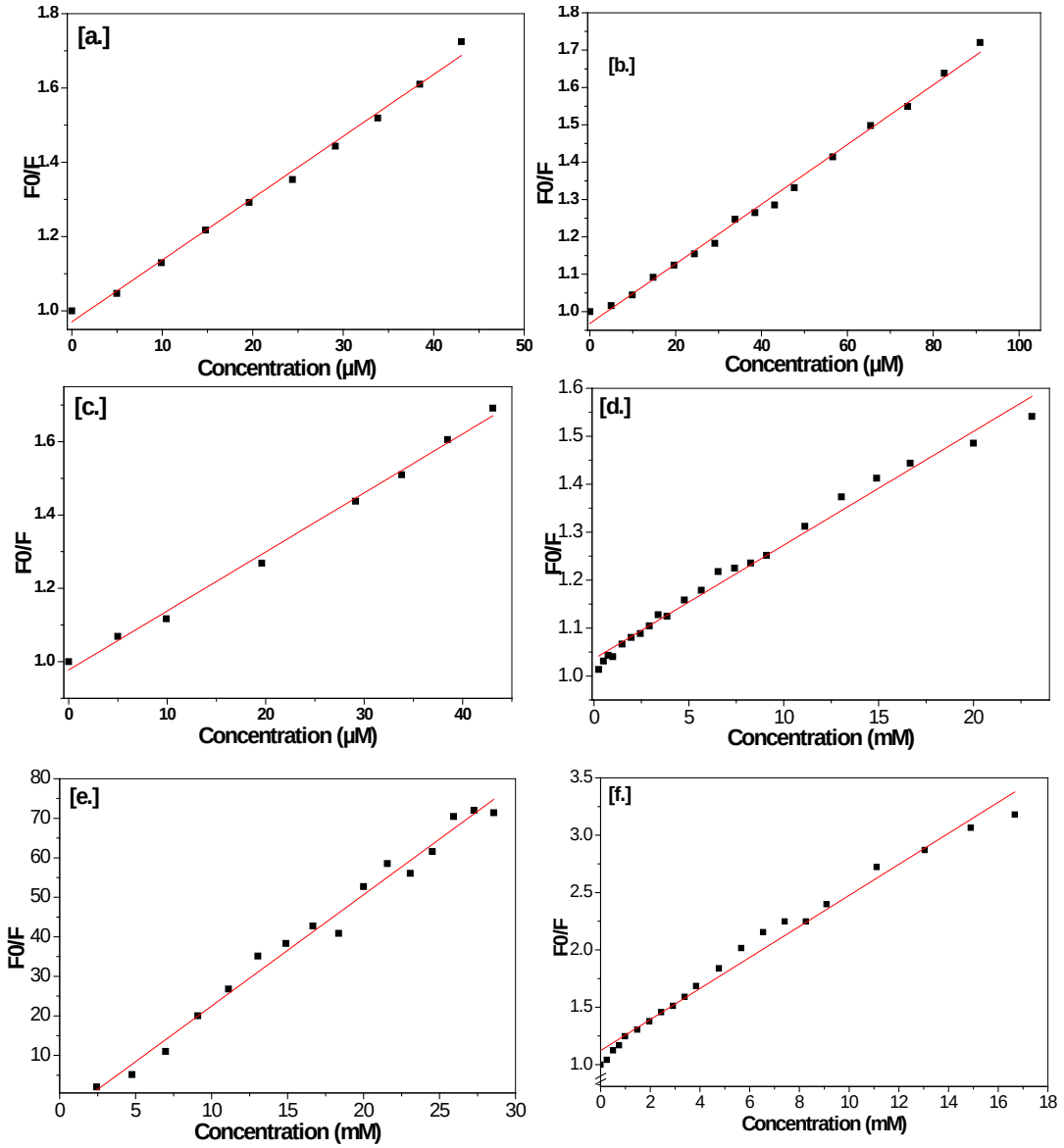

Figure 4.11 Linearity graph (stern-volmer) for quenching study (a-f) of CQDs with (a) 4-NP (b) DNP (C) TNP (d) 4-CP (e) MnCP (f) Phenol

It was observed from the results that Nitrophenols were better detected as compared to other analytes under study (Figure 4.12).

Table 4.2 Results from the Stern-Volmer equation applied to the study

Model pollutants	**Quenching Constant (M^{-1})**	**R^2 value**
4-NP	16646	0.9931
DNP	7983	0.9948
TNP	16094	0.9924
4-CP	23.7	0.9864
MnCP	280	0.9844
Phenol	135	0.9829

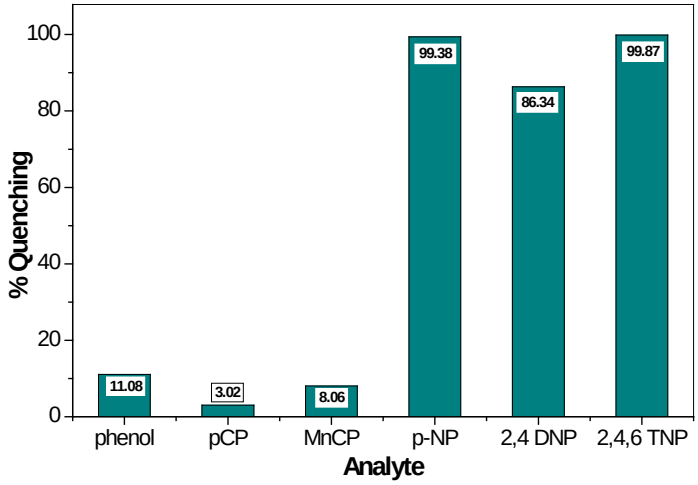

Figure 4.12 Comparison of quenching of CQDs fluorescence in presence of analytes [(Excitation at 310 nm, Emission at 410 nm); 2ml CQDs+ 497.5 µM pollutants]

PART-B

(Graphene Quantum Dots prepared from DTPA)

4.4 Experimental

4.4.1 Chemicals and precursor

DTPA (Diethylenetriaminepentaacetic acid Spectrochem India, AR grade), Ethyl acetate (LR grade, Spectrochem) were used. Other chemical used have been mentioned in section 4.2.1.

4.4.2 Preparation of GQDs

The synthesis of GQDs was carried out by a simple hydro-thermal treatment of DTPA as depicted in figure 4.13. In a typical preparation, 0.2 g of DTPA was dissolved in 20 mL 1% NaOH aqueous solution; the clear solution was stirred for 15-20 min to ensure complete homogeneity. The solution was then transferred to an evaporating dish and was thermally treated in an oven at 200°C for 8 h. The clear solution changed to light brown colored mass, which was dissolved in water and made up to 100 mL with water. The obtained yellowish-brown colored solution was then centrifuged at 10000 rpm for 10 min to remove heavier particles if present. The resulting yellowish brown color solution contained GQDs and was purified using dialysis membrane (6000-8000 Da). The separated and purified GQDs were characterized. The probable structure of GQDs is hypothetically depicted in figure 4.14.

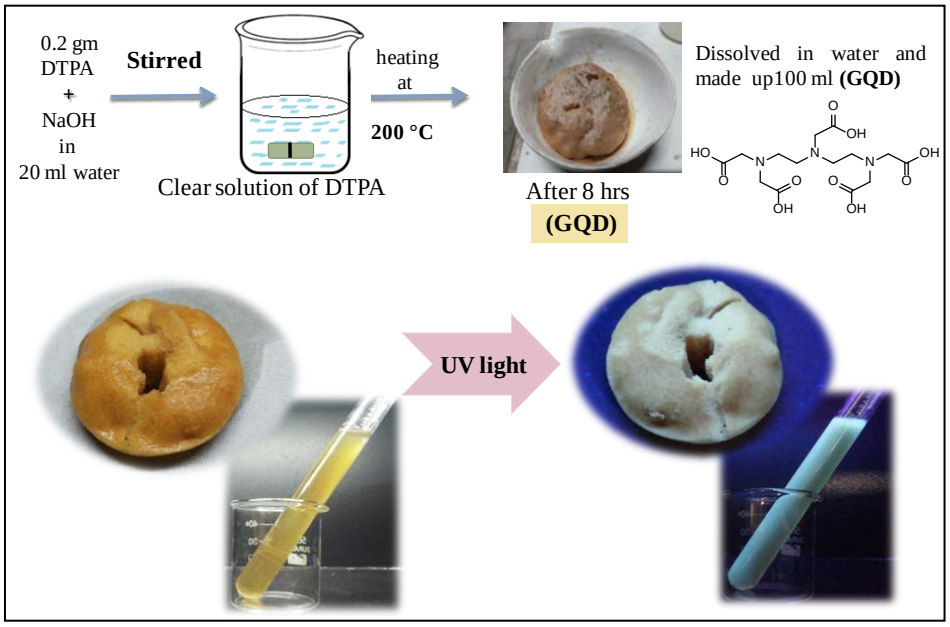

Figure 4.13 Scheme for the preparation of GQDs

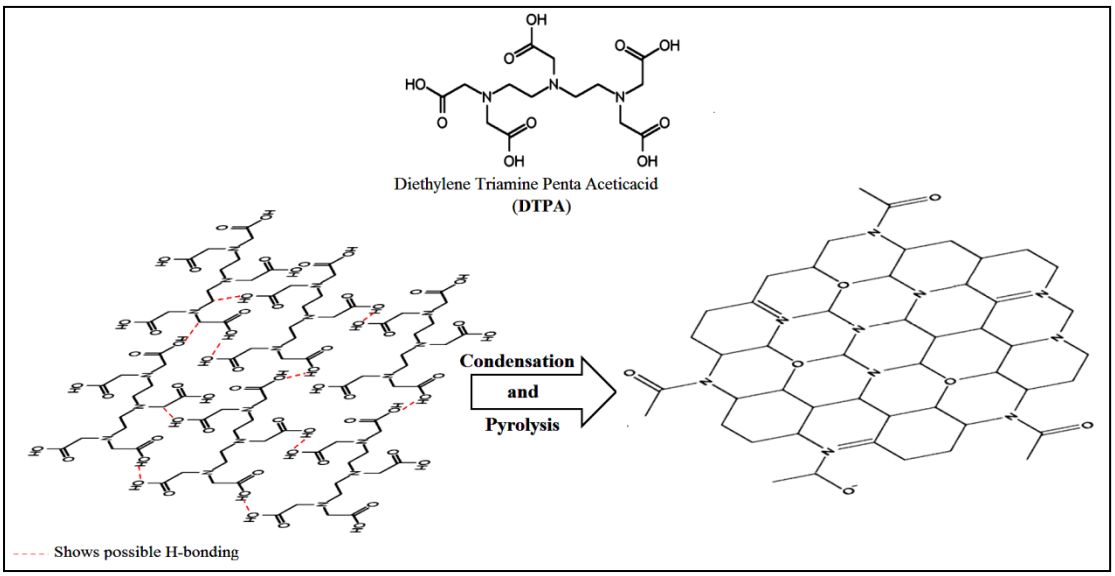

Figure 4.14 plausible pathways for the formation of GQDs

(Adopted from mechanism suggested by (Arvand and Hemmati, 2017))

4.4.3 Characterisation of GQDs

The prepared GQDs were characterized by TEM, Raman, FTIR, UV-Visible and fluorescence spectroscopic techniques.

4.4.4 GQDs as sensor for Model Pollutants

Sensing study of the prepared GQDs for model pollutants were carried out using fluorescence measurements. In a typical experiment 2 ml of 10% aqueous solution of GQDs (W/V) solution was measured for initial fluorescence intensity. Sensing study was carried out by successive addition of known concentration of analyte , followed by measuring fluorescence after excitation at 365 nm. The excitation wavelength and pH was optimized before sensing study carried out.

4.5 Results and discussions

4.5.1 Characterizations of GQDs

4.5.1.1 TEM analysis

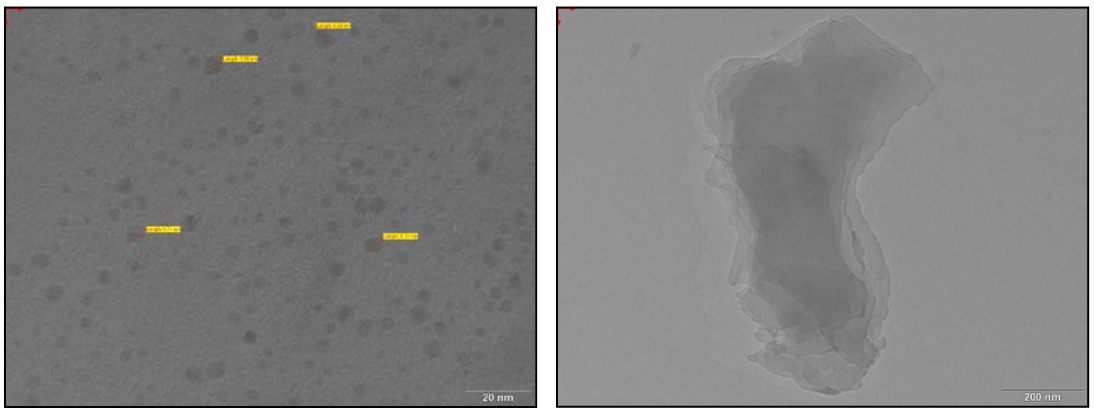

Figure 4.15 TEM images of GQDs

TEM studies revealed that the GQDs consisted of a few layers with sizes in the range 3-7 nm with wrinkles at the edges (Figure 4.15). To the best of our knowledge multilayer graphene quantum dots have only been reported by Dong et al. prepared from carbon black (Dong et al., 2012a).

4.5.1.2 FTIR analysis

The FTIR spectra of DTPA and GQDs are shown in figure 4.16

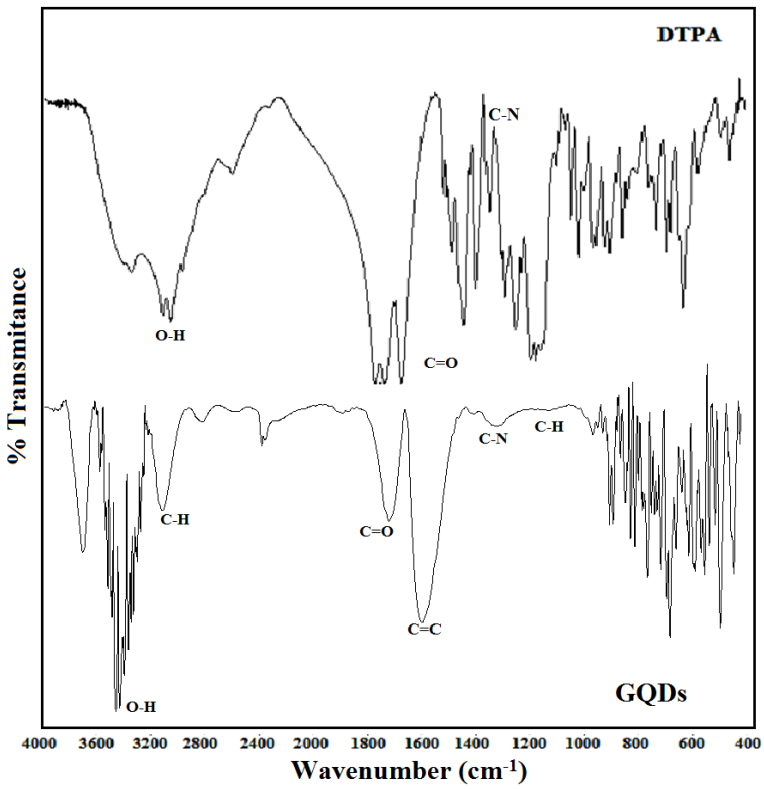

Figure 4.16 FTIR spectra of DTPA and GQDs

The sharp bands at~ 3350 cm^{-1} and 3150 cm^{-1} corresponded to the stretching vibrations of O−H groups, while the peak centred at~2900 cm^{-1} is typically associated with sp^3 C−H stretching vibrations (Figure 4.16). C-N stretching vibration was observed at~1400 cm^{-1}, while C-H vibration was observed at 1100 cm^{-1}.Two separate peaks were observed around 1600 cm^{-1} and 1700 cm^{-1} attributed to C=O and C=C stretching vibrations respectively. The IR spectral analysis thus indicated that the GQDs contained -CH_2-, -OH and -COOH and -NH_2 groups. These groups could also be responsible for a strong hydrophilic nature of the synthesized GQDs

4.5.1.3 Raman analysis

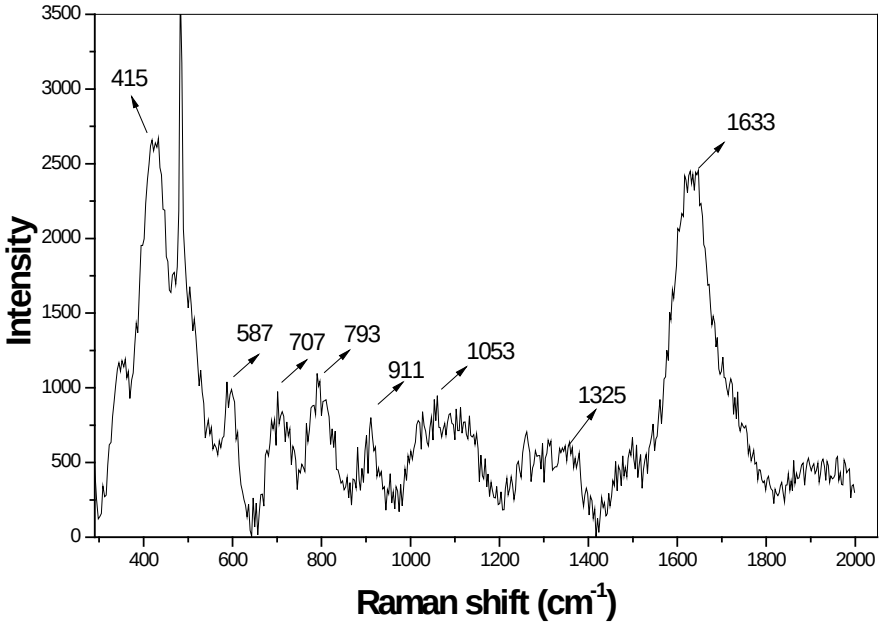

Figure 4.17 Raman spectra of GQDs

As shown in Figure 4.17 the Raman spectrum of GQDs exhibits a band at~1325 cm^{-1} and an intense band at~1633 cm^{-1}, which can be attributed to D-band (sp^3) and G-band (sp^2) respectively. The intense G band could be arising from the small sp^2 cluster size (Roushani et al., 2015; Zhang M. et al., 2012).The I_d/I_g ratio was 0.096, which corresponds to graphitic structures of quantum dots. The G band is at a higher wavenumber due to high amounts of carbon bonded to either neighboring carbon or with oxygen in the form of hydroxyl group via sp^3 hybridization (Kudin et al., 2008; Umrao et al., 2015). The G band is of strong intensity indicating the ordered nature of the observed GQDs with fewer defects and the structure is similar to that of graphite and is highly crystalline (Shi B. et al., 2015). Since the GQDs are already functionalized with -COOH, an increase in the D:G ratio is not expected and was also

not observed by Achadu et al. (Achadu et al., 2016). Two peaks were observed in the low frequency region as observed for GQDs attributed to bending modes of sp linear structures and some amorphous sp^3 bonded carbon.

4.5.1.4 Zeta Potential measurements

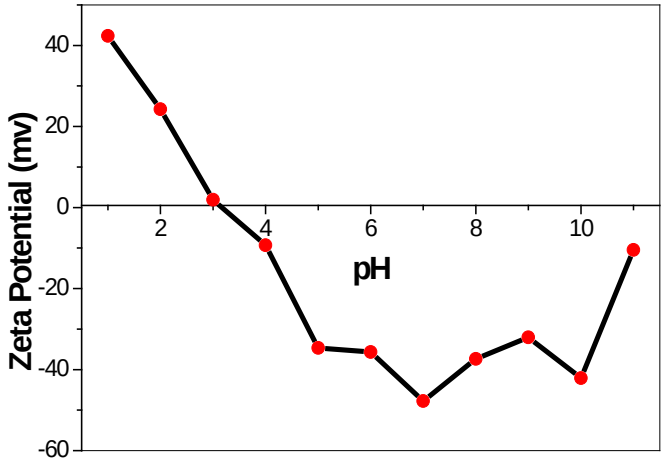

Figure 4.18 Zeta-potential analysis of GQDs

Zeta potential of this solution was measured to be ca. -47.8 mV (at pH 7) indicating the formation of highly negative charged surface and well dispersed GQDs with effective stability (Figure 4.18). Measurement of zeta potential against pH shows that at low pH zeta potential is positive (+42.36 mV) which shifts to negative at higher pH indicating the presence of –C=O groups on the surface (Lin et al., 2015). The pH_{ZPC} was found to be 3.1.

4.5.2 UV absorption and Photoluminescence studies

The formation of GQDs was investigated by measuring the fluorescence spectra and UV–Vis absorption spectra. Figures 4.19 (a) and (b) depict the UV−visible absorption and fluorescence emission spectra respectively. The prepared GQDs exhibited an absorption shoulder at~272 nm which was attributed to n-π* transition of C=O (Yang et al., 2014) and another weak shoulder at~340 nm can be attributed to n-π* transition of C=N.

The prepared GQDs as well as its suspension exhibited a blue coloured fluorescence which could be observed with the naked eye under ultraviolet radiation (Figure 4.19 (a)).

The aqueous GQD solution exhibited a fluorescence emission band at~454 nm when excited at 365 nm. The fluorescence was a clear evidence of the formation of GQDs. During the heating process, neighboring dehydrated DTPA molecules react with each

other to form GQDs, and the functional groups, such as -OH,-NH_2, -CH_2, -COOH, and -COOR, located at the edge of each GQDs passivated the GQD layers facilitating the uniform dispersion of the sp^2 clusters in the GQD structure (Li et al., 2015).

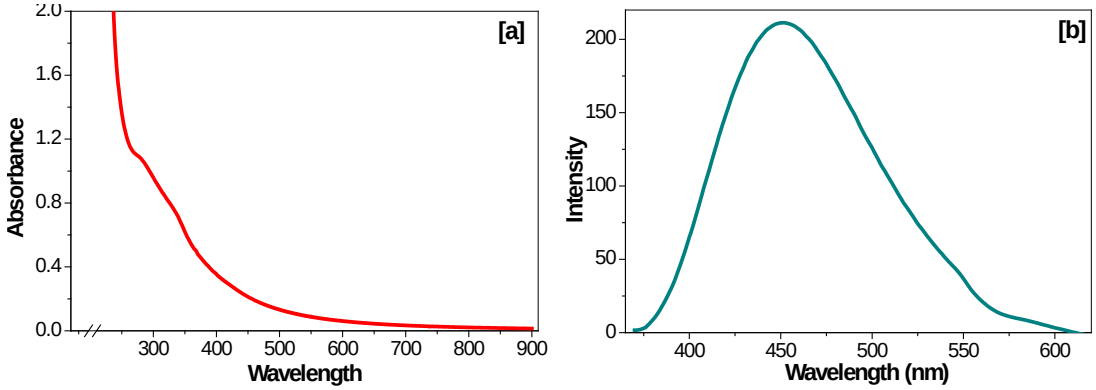

Figure 4.19 GQDs (a) Absorption spectra (b) Emission spectra

The quantum yield was calculated to be about 2.32% using quinine sulfate in 0.1 M sulphuric acid as the standard, while Dong et al. reported 4.04% for multilayer graphene quantum dots using Rhodamine 6G as standard (Dong et al., 2012b).

4.5.3. Optimisation of fluorescence of GQDs

4.5.3.1 Effect of Excitation wavelength

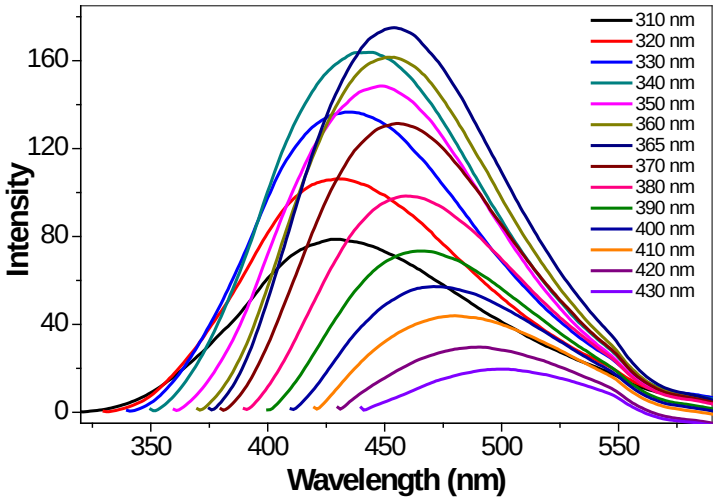

Figure 4.20 Emission spectra of GQDs with Excitation wavelength varying from 310 to 430 nm)

The photoluminescence was excitation independent when the excitation wavelength was lower than 400 nm, but shifted from ~ 450 nm to ~ 500 nm when the excitation wavelength was changed from 400 nm to 430 nm as seen from Figure 4.20. Similar excitation independent photoluminescence behavior was also observed by Dong et al. when excitation wavelength was lower than 400 nm. However emission intensity increased with increase in excitation wavelength below 400 nm. Further another

emission shoulder was observed at ~ 560 nm when excited at 340 nm which shifted to longer wavelengths with increase in excitation wavelengths. A similar phenomenon of multiple emissive states was observed by Dhenadayalan et al. in citric acid derived carbon dots and the phenomenon was attributed to different surface states of the carbon dots (Dhenadhayalan et al., 2016). The fluorescence emission by GQDs can be attributed to the radiative recombination of excitons which are trapped by the defects arising during synthesis (Bourlinos et al., 2008; Peng and Travas-Sejdic, 2009; Ray et al., 2009; Sun et al., 2006; Yang et al., 2012). Further, the presence of nanosized sp^2 domains due to abundant -COOH functional groups at the surface of GQDs also cause charge confinement leading to the photoluminescence properties of GQDs (Sun et al., 2013).

4.5.3.2 Effect of pH on fluorescence intensity of GQDs

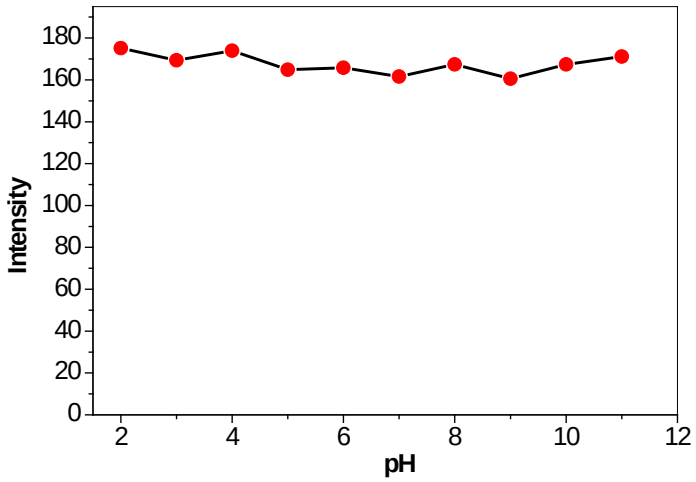

Figure 4.21 Effect of pH on fluorescence intensity of GQDs

A number of studies have shown that the pH of the medium strongly influences the fluorescence of GQDs (Liu et al., 2012; Wee et al., 2013). The pH of the GQDs solution was adjusted by using 0.1 N HCl and 0.1 N NaOH solutions. From the pH variation study (Figure 4.21), it was observed that the intensity of fluorescence was not affected much with pH. So a neutral pH 6-7 was selected for further experiments.

4.5.4 Sensing studies

The GQDs were used for quantitative sensing of the model pollutants under study. The fluorescence intensity of the GQDs was gradually quenched upon the addition of increasing concentration of the analytes under study (Figure 4.22). It was observed that maximum fluorescence quenching (≥ 99.8 %) was achieved by 4-NP, DNP and

TNP at concentrations of 2.44 mM, 6.98 mM and 0.74 mM respectively while phenol, 4-CP and MnCP did not give such fluorescence quenching.

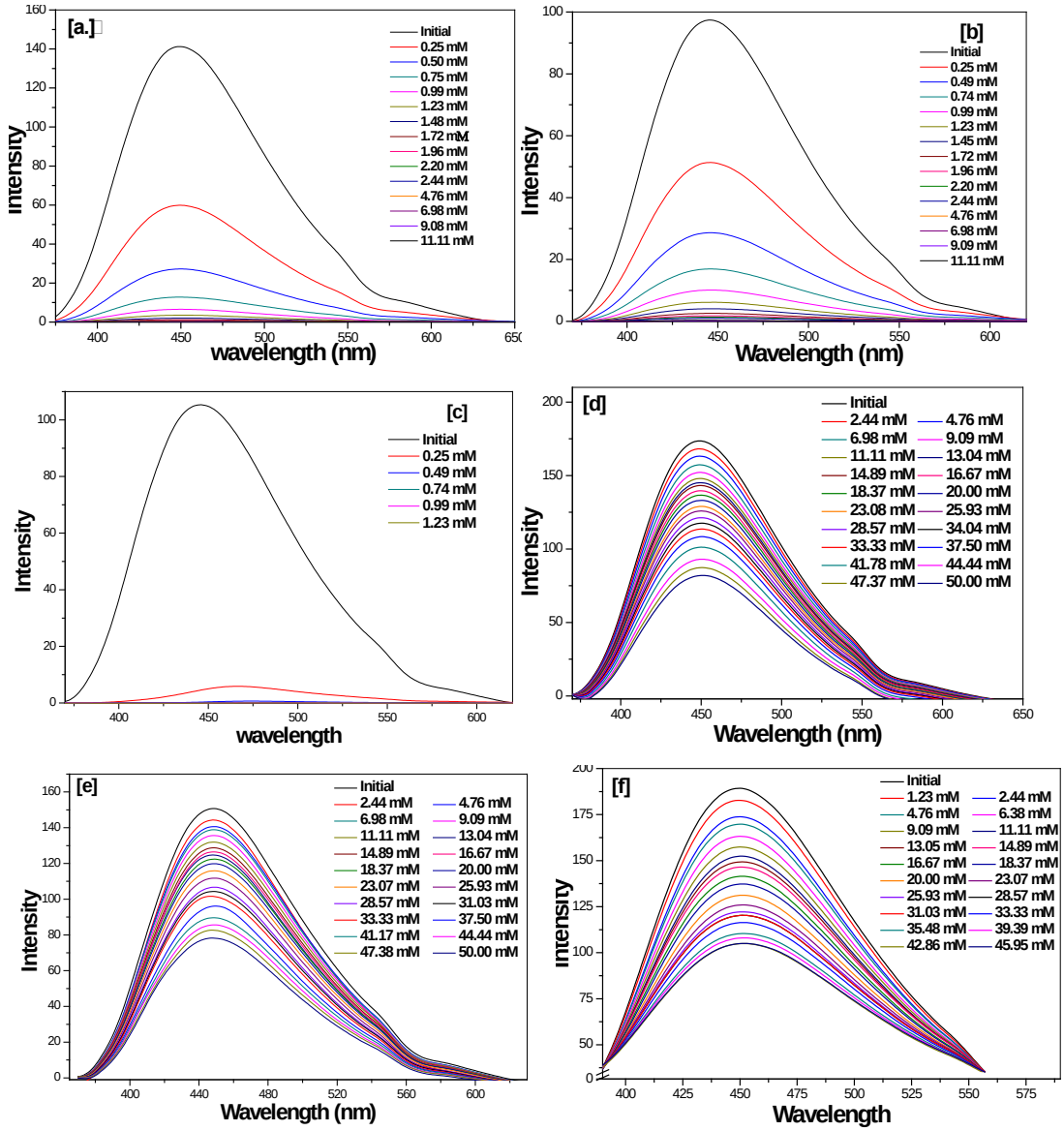

Figure 4.22 Fluorescence spectra of GQDs in the presence of
(a) 4-NP (b) DNP (C) TNP (d) 4-CP (e) MnCP (f) Phenol

The performance of the GQDs were analysed by using the Stern-Volmer equation. The K_{SV} values obtained from the slope (Table 4.3), as well as the detection limit of analytes (Table 4.3) indicated that sensing of nitrophenols was most effective as compared to phenol, CP and MnCP using GQDs (Figure 4.23 and Figure 4.24).

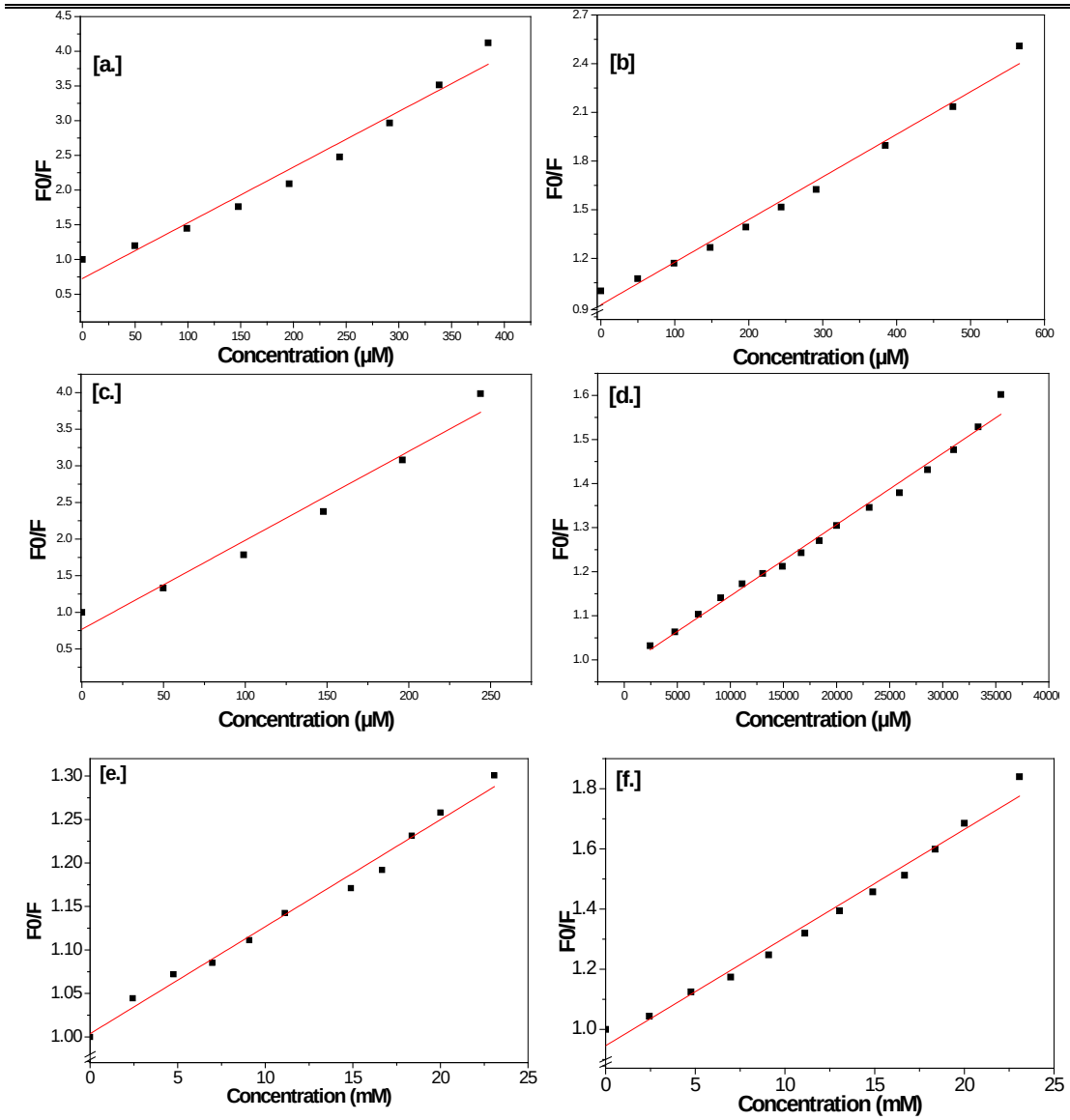

Figure 4.23 Linearity graph of quenching study (a-f) of GQDs with (a) 4-NP (b) DNP (C) TNP (d) 4-CP (e) MnCP (f) Phenol

Table 4.3 Results from the Stern-Volmer equation applied to the study

Analyte	**Quenching Constant (M^{-1})**	**R^2**
4-NP	7348	0.9624
DNP	2625	0.9851
TNP	12147	0.9617
p-CP	16.23	0.9907
MnCP	12.32	0.9869
Phenol	359.1	0.9829

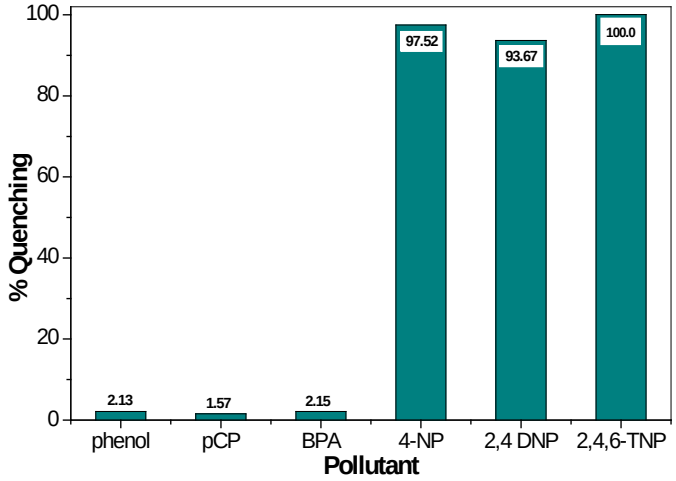

Figure 4.24 Comparison of quenching of GQDs fluorescence in presence of analytes under study

[(Excitation at 365 nm, Emission at 450 nm); 2mL GQDs +1234.5 µM pollutants; Intensity Measured at Excitation at 365 nm Emission wavelength 450 nm]

4.5.5 Reusability study

The reusability of GQDs was carried out by extraction of analyte under study (Nitrophenols) with ethyl acetate (EA). After recovery of analyte, the GQDs could be reused for sensing study.

The recovery of analyte was studied systematically by taking different amount of EA 1-7 mL to a fixed amount of GQDs and analyte, where maximum quenching was achieved. It was found that the 7 mL of EA was required to obtain 76.8-% recovery (Figure 4.25). However, we were not successful in recovering nitrophenol from CQDs

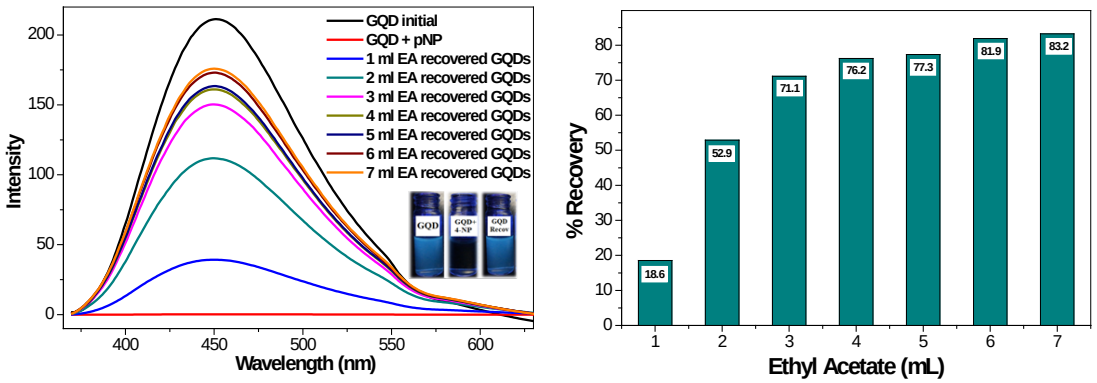

Figure 4.25 Recovery study optimisation

GQD solution- 4 mL, 4-NP=11.11 mM, pH=6

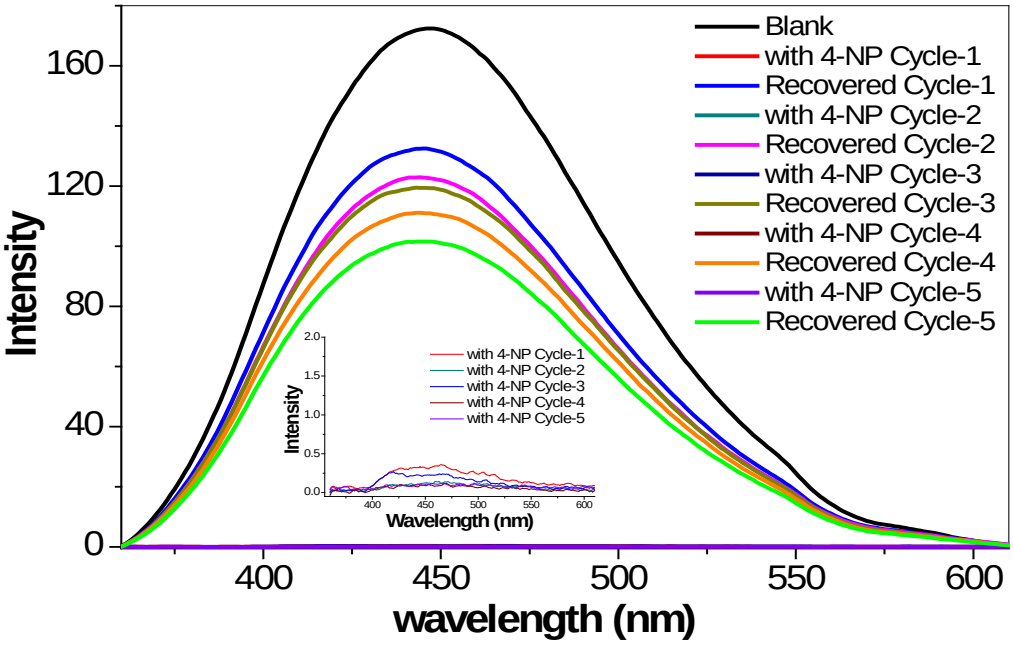

Figure 4.26 (a) Reusability of GQDs where the Graph shows the fluorescence spectra of pristine GQDS and recovered GQDS after 1st to 5th cycle while inset shows spectra of GQD + 4-NP after 1st to 5th cycle

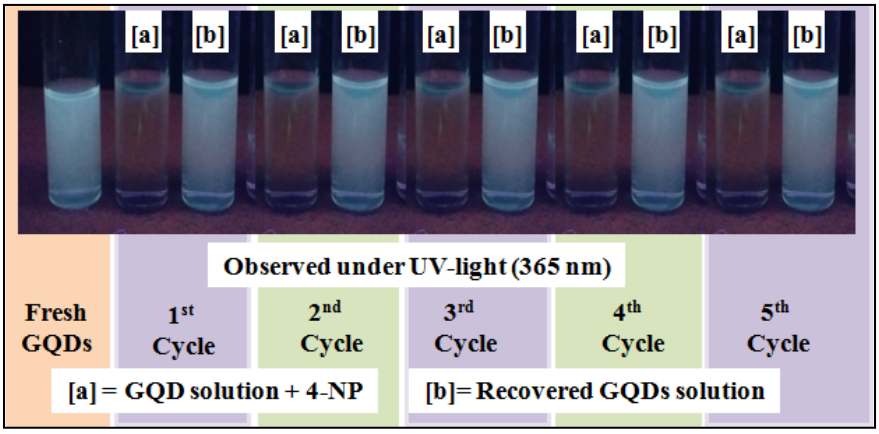

Figure 4.26 (b) Reusability of GQDs

The reusability was tested up to five cycles (Figure 4.26 (a and b)). The GQDs were effective for sensing of 4-NP.

The validation parameters for the detection methods of nitrophenols using CDs and GQDs developed in this study were investigated and compared with literature reported values (Table 4.4). The LOD values were comparable with literature reported CDs and GQDs and the response was linear over a wide range as compared to other reported CDs and GQDs.

Table 4.4 Comparison table with reported nanodots sensors for nitrophenols

Sensor	NPs	LOD µm	LOQ µm	Linear range µm	References
Fluorescence quenching of nano-carbon	4-NP	0.028	0.092	0.1–50	Ahmed et al., 2015
MIP-coated GQDs fluorescent sensor	4-NP	9.0	29.70	0.02–3.00	Zhou et al., 2014
$Ru(bpy)_3^{2+}$–Ce(IV) -GQDs CL system	4-NP	0.03	0.099	0.1–2.5	Amjadi and Hallaj, 2016
N-doped Carbon dots from maleic acid	4-NP	0.16	0.528	0.72 – 79	Yuan et al., 2016
Carbon Dots induced by acetone passivation	DNP	400	1320	0.001-0.010	Cayuela et al., 2013
Citric acid based GQDs	TNP	0.091	0.3003	0.1- 15	Li et al., 2015
Conducting Carbon Dot – Polypyrrole Nanocomposite	TNP	0.14	0.462	0.50-15.0	Pal et al., 2016
P-doped carbon dots	TNP	0.016	0.0528	0.2-17.0	Shi D. et al., 2015
Citric acid based nitrogen-doped grapheme quantum dots	TNP	0.30	0.99	1 to 60	Lin et al., 2015
Palmshell based carbon dots (CQDs)	4-NP	0.079	0.237	0.2-40	Present study
	DNP	0.165	0.494	0.5-85	
	TNP	0.082	0.245	0.2-40	
DTPA based Graphene quantum dots (GQDs)	4-NP	0.154	0.462	0.5-350	Present study
	DNP	0.430	1.289	1.3-500	
	TNP	0.093	0.278	0.3-210	

4.6 Conclusions

In conclusion, we have demonstrated a facile synthesis of CQDs and GQDs by chemical exfoliation of triflic acid activated PSP and by hydrothermal treatment of DTPA respectively, which are rich in distributed graphitic domains. The strategy of using triflic acid for the preparation of CQDs has been attempted for the first time. Similarly this is the first attempt reported for the synthesis of multilayered GQDs using DTPA as precursor. The CQDs and GQDs emitted strong and stable green and blue fluorescence at a quantum yield of 0.98 and 2.32% respectively, the fluorescence of synthesized CQDs and GQDs was efficiently quenched by Nitro compounds and hence was effective in sensing NPs (4-NP, DNP and TNP). The quenching in fluorescence during interaction of the NPs with CQDs and GQDs could be due to strong π-π* stacking interactions. The efficiency of the as prepared CQDs and GQDs were comparable with other quantum dots available in literature for sensing nitrophenols.

4.7 References

Achadu, O.J., Uddin, I., Nyokong, T., 2016. Fluorescence behavior of nanoconjugates of graphene quantum dots and zinc phthalocyanines. J. Photochem. Photobiol. A Chem. 317, 12–25. doi:http://dx.doi.org/10.1016/j.jphotochem.2015.11.006

Ahmed, G.H.G., Laíño, R.B., Calzón, J.A.G., García, M.E.D., 2015. Highly fluorescent carbon dots as nanoprobes for sensitive and selective determination of 4-nitrophenol in surface waters. Microchim. Acta 182, 51–59. doi:10.1007/s00604-014-1302-x

Amjadi, M., Hallaj, T., 2016. Dramatic enhancement effect of carbon quantum dots on the chemiluminescence of –Ce(IV) reaction and application to the determination of 4-nitrophenol. J. Lumin. 171, 202–207. doi:http://dx.doi.org/10.1016/j.jlumin.2015.11.019

Arvand, M., Hemmati, S., 2017. Magnetic nanoparticles embedded with graphene quantum dots and multiwalled carbon nanotubes as a sensing platform for electrochemical detection of progesterone. Sensors Actuators B Chem. 238, 346–356. doi:http://dx.doi.org/10.1016/j.snb.2016.07.066

Baker, S.N., Baker, G.A., 2010. Luminescent Carbon Nanodots: Emergent Nanolights. Angew. Chemie Int. Ed. 49, 6726–6744. doi:10.1002/anie.200906623

Bao, L., Zhang, Z.-L., Tian, Z.-Q., Zhang, L., Liu, C., Lin, Y., Qi, B., Pang, D.-W., 2011. Electrochemical tuning of luminescent carbon nanodots: from preparation to luminescence mechanism. Adv. Mater. 23, 5801–5806. doi:10.1002/adma.201102866

Bourlinos, A.B., Stassinopoulos, A., Anglos, D., Zboril, R., Karakassides, M., Giannelis, E.P., 2008. Surface Functionalized Carbogenic Quantum Dots. Small 4, 455–458. doi:10.1002/smll.200700578

Casari, C.S., Li Bassi, A., Baserga, A., Ravagnan, L., Piseri, P., Lenardi, C.,

Tommasini, M., Milani, A., Fazzi, D., Bottani, C.E., Milani, P., 2008. Low-frequency modes in the Raman spectrum of sp-sp^2 nanostructured carbon. Phys. Rev. B 77, 195444. doi:10.1103/PhysRevB.77.195444

Cayuela, A., Soriano, M.L., Valcárcel, M., 2013. Strong luminescence of Carbon Dots induced by acetone passivation: Efficient sensor for a rapid analysis of two different pollutants. Anal. Chim. Acta 804, 246–251. doi:http://dx.doi.org/10.1016/j.aca.2013.10.031

Dai, H., Shi, Y., Wang, Y., Sun, Y., Hu, J., Ni, P., Li, Z., 2014. A carbon dot based biosensor for melamine detection by fluorescence resonance energy transfer. Sensors Actuators B Chem. 202, 201–208. doi:http://dx.doi.org/10.1016/j.snb.2014.05.058

De, B., Karak, N., 2013. A green and facile approach for the synthesis of water soluble fluorescent carbon dots from banana juice. RSC Adv. 3, 8286–8290. doi:10.1039/C3RA00088E

Dhenadhayalan, N., Lin, K.-C., Suresh, R., Ramamurthy, P., 2016. Unravelling the Multiple Emissive States in Citric-Acid-Derived Carbon Dots. J. Phys. Chem. C 120, 1252–1261. doi:10.1021/acs.jpcc.5b08516

Dong, Y., Chen, C., Zheng, X., Gao, L., Cui, Z., Yang, H., Guo, C., Chi, Y., Li, C.M., 2012a. One-step and high yield simultaneous preparation of single- and multi-layer graphene quantum dots from CX-72 carbon black. J. Mater. Chem. 22, 8764–8766. doi:10.1039/C2JM30658A

Dong, Y., Pang, H., Yang, H. Bin, Guo, C., Shao, J., Chi, Y., Li, C.M., Yu, T., 2013. Carbon-Based Dots Co-doped with Nitrogen and Sulfur for High Quantum Yield and Excitation-Independent Emission. Angew. Chemie Int. Ed. 52, 7800–7804. doi:10.1002/anie.201301114

Dong, Y., Shao, J., Chen, C., Li, H., Wang, R., Chi, Y., Lin, X., Chen, G., 2012b. Blue luminescent graphene quantum dots and graphene oxide prepared by tuning the carbonization degree of citric acid. Carbon, 50, 4738–4743.

doi:http://dx.doi.org/10.1016/j.carbon.2012.06.002

Dong, Y., Wan, L., Cai, J., Fang, Q., Chi, Y., Chen, G., 2015. Natural carbon-based dots from humic substances. Sci. Rep. 5, 10037.

Dong, Y., Zhou, N., Lin, X., Lin, J., Chi, Y., Chen, G., 2010. Extraction of electrochemiluminescent oxidized carbon quantum dots from activated carbon. Chem. Mater. 22, 5895–5899. doi:10.1021/cm1018844

Du, F., Zhang, M., Li, X., Li, J., Jiang, X., Li, Z., Hua, Y., Shao, G., Jin, J., Shao, Q., Zhou, M., Gong, A., 2014. Economical and green synthesis of bagasse-derived fluorescent carbon dots for biomedical applications. Nanotechnology 25, 315702. doi:10.1088/0957-4484/25/31/315702

Dubey, P., Tripathi, K.M., Mishra, R., Bhati, A., Singh, A., Sonkar, S.K., 2015. A simple one-step hydrothermal route towards water solubilization of carbon quantum dots from soya-nuggets for imaging applications. RSC Adv. 5, 87528–87534. doi:10.1039/C5RA14536H

Essig, S., Marquardt, C.W., Vijayaraghavan, A., Ganzhorn, M., Dehm, S., Hennrich, F., Ou, F., Green, A.A., Sciascia, C., Bonaccorso, F., Bohnen, K.-P., Lohneysen, H. v, Kappes, M.M., Ajayan, P.M., Hersam, M.C., Ferrari, A.C., Krupke, R., 2010. Phonon-assisted electroluminescence from metallic carbon nanotubes and graphene. Nano Lett. 10, 1589–1594. doi:10.1021/nl9039795

Fan, L., Hu, Y., Wang, X., Zhang, L., Li, F., Han, D., Li, Z., Zhang, Q., Wang, Z., Niu, L., 2012. Fluorescence resonance energy transfer quenching at the surface of graphene quantum dots for ultrasensitive detection of TNT. Talanta 101, 192–197. doi:http://dx.doi.org/10.1016/j.talanta.2012.08.048

Ferrari, A.C., Robertson, J., 2004. Raman spectroscopy of amorphous, nanostructured, diamond like carbon, and nanodiamond. Philos. Trans. R. Soc. London A Math. Phys. Eng. Sci. 362, 2477–2512. doi:10.1098/rsta.2004.1452

Geim, A.K., Novoselov, K.S., 2007. The rise of graphene. Nat Mater 6, 183–191.

Gu, J., Hu, M.J., Guo, Q.Q., Ding, Z.F., Sun, X.L., Yang, J., 2014. High-yield synthesis of graphene quantum dots with strong green photoluminescence. RSC Adv. 4, 50141–50144. doi:10.1039/C4RA10011E

Güttinger, J., Molitor, F., Stampfer, C., Schnez, S., Jacobsen, A., Dröscher, S., Ihn, T., Ensslin, K., 2012. Transport through graphene quantum dots. Reports Prog. Phys. 75, 126502.

Himaja, A.L., Karthik, P.S., Sreedhar, B., Singh, S.P., 2014. Synthesis of carbon dots from kitchen waste: conversion of waste to value added product. J. Fluoresc. 24, 1767–1773. doi:10.1007/s10895-014-1465-1

Hu, B., Wang, K., Wu, L., Yu, S.-H., Antonietti, M., Titirici, M.-M., 2010. Engineering Carbon Materials from the Hydrothermal Carbonization Process of Biomass. Adv. Mater. 22, 813–828. doi:10.1002/adma.200902812

Hu, C., Liu, Y., Yang, Y., Cui, J., Huang, Z., Wang, Y., Yang, L., Wang, H., Xiao, Y., Rong, J., 2013. One-step preparation of nitrogen-doped graphene quantum dots from oxidized debris of graphene oxide. J. Mater. Chem. B 1, 39–42. doi:10.1039/C2TB00189F

Hu, S., Wei, Z., Chang, Q., Trinchi, A., Yang, J., 2016. A facile and green method towards coal-based fluorescent carbon dots with photocatalytic activity. Appl. Surf. Sci. 378, 402–407. doi:http://dx.doi.org/10.1016/j.apsusc.2016.04.038

Huang, Y., Dong, X., Liu, Y., Li, L.-J., Chen, P., 2011. Graphene-based biosensors for detection of bacteria and their metabolic activities. J. Mater. Chem. 21, 12358–12362. doi:10.1039/C1JM11436K

Jia, X., Li, J., Wang, E., 2012. One-pot green synthesis of optically pH-sensitive carbon dots with upconversion luminescence. Nanoscale 4, 5572–5575. doi:10.1039/C2NR31319G

Jin, S.H., Kim, D.H., Jun, G.H., Hong, S.H., Jeon, S., 2013. Tuning the photoluminescence of graphene quantum dots through the charge transfer effect of functional groups. ACS Nano 7, 1239–1245. doi:10.1021/nn304675g

Kasibabu, B.S.B., D'souza, S.L., Jha, S., Kailasa, S.K., 2015. Imaging of Bacterial and Fungal Cells Using Fluorescent Carbon Dots Prepared from Carica papaya Juice. J. Fluoresc. 25, 803–810. doi:10.1007/s10895-015-1595-0

Krysmann, M.J., Kelarakis, A., Dallas, P., Giannelis, E.P., 2012. Formation mechanism of carbogenic nanoparticles with dual photoluminescence emission. J. Am. Chem. Soc. 134, 747–750. doi:10.1021/ja204661r

Kudin, K.N., Ozbas, B., Schniepp, H.C., Prud'homme, R.K., Aksay, I.A., Car, R., 2008. Raman spectra of graphite oxide and functionalized graphene sheets. Nano Lett. 8, 36–41. doi:10.1021/nl071822y

Kumar Singh, K., Verma, V., Bhatti, H.S., D., 2014. Synthesis and characterization of carbon quantum dots from orange juice. J. Bionanoscience 8, 274–279. doi:10.1166/jbns.2014.1236

Li, H., He, X., Liu, Y., Huang, H., Lian, S., Lee, S.-T., Kang, Z., 2011. One-step ultrasonic synthesis of water-soluble carbon nanoparticles with excellent photoluminescent properties. Carbon N. Y. 49, 605–609. doi:http://dx.doi.org/10.1016/j.carbon.2010.10.004

Li, L.-L., Ji, J., Fei, R., Wang, C.-Z., Lu, Q., Zhang, J.-R., Jiang, L.-P., Zhu, J.-J., 2012. A Facile Microwave Avenue to Electrochemiluminescent Two-Color Graphene Quantum Dots. Adv. Funct. Mater. 22, 2971–2979. doi:10.1002/adfm.201200166

Li, Q., Zhang, S., Dai, L., Li, L., 2012. Nitrogen-doped colloidal graphene quantum dots and their size-dependent electrocatalytic activity for the oxygen reduction reaction. J. Am. Chem. Soc. 134, 18932–18935. doi:10.1021/ja309270h

Li, W., Zhang, Z., Kong, B., Feng, S., Wang, J., Wang, L., Yang, J., Zhang, F., Wu, P., Zhao, D., 2013. Simple and Green Synthesis of Nitrogen-Doped Photoluminescent Carbonaceous Nanospheres for Bioimaging. Angew. Chemie Int. Ed. 52, 8151–8155. doi:10.1002/anie.201303927

Li, Y., Hu, Y., Zhao, Y., Shi, G., Deng, L., Hou, Y., Qu, L., 2011. An

Electrochemical Avenue to Green-Luminescent Graphene Quantum Dots as Potential Electron-Acceptors for Photovoltaics. Adv. Mater. 23, 776–780. doi:10.1002/adma.201003819

Li, Y., Zhao, Y., Cheng, H., Hu, Y., Shi, G., Dai, L., Qu, L., 2012. Nitrogen-doped graphene quantum dots with oxygen-rich functional groups. J. Am. Chem. Soc. 134, 15–18. doi:10.1021/ja206030c

Li, Z., Wang, Y., Ni, Y., Kokot, S., 2015. A sensor based on blue luminescent graphene quantum dots for analysis of a common explosive substance and an industrial intermediate, 2,4,6-trinitrophenol. Spectrochim. Acta. A. Mol. Biomol. Spectrosc. 137, 1213–1221. doi:10.1016/j.saa.2014.09.009

Liang, Q., Ma, W., Shi, Y., Li, Z., Yang, X., 2013. Easy synthesis of highly fluorescent carbon quantum dots from gelatin and their luminescent properties and applications. Carbon N. Y. 60, 421–428. doi:http://dx.doi.org/10.1016/j.carbon.2013.04.055

Lin, L., Rong, M., Lu, S., Song, X., Zhong, Y., Yan, J., Wang, Y., Chen, X., 2015. A facile synthesis of highly luminescent nitrogen-doped graphene quantum dots for the detection of 2,4,6-trinitrophenol in aqueous solution. Nanoscale 7, 1872–1878. doi:10.1039/C4NR06365A

Lin, L., Zhang, S., 2012. Creating high yield water soluble luminescent graphene quantum dots via exfoliating and disintegrating carbon nanotubes and graphite flakes. Chem. Commun. 48, 10177–10179. doi:10.1039/C2CC35559K

Lin, X., Gao, G., Zheng, L., Chi, Y., Chen, G., 2014. Encapsulation of strongly fluorescent carbon quantum dots in metal-organic frameworks for enhancing chemical sensing. Anal. Chem. 86, 1223–1228. doi:10.1021/ac403536a

Liu, H., Ye, T., Mao, C., 2007. Fluorescent Carbon Nanoparticles Derived from Candle Soot. Angew. Chemie Int. Ed. 46, 6473–6475. doi:10.1002/anie.200701271

Liu, J.-M., Lin, L., Wang, X.-X., Lin, S.-Q., Cai, W.-L., Zhang, L.-H., Zheng, Z.-Y.,

2012. Highly selective and sensitive detection of Cu^{2+} with lysine enhancing bovine serum albumin modified-carbon dots fluorescent probe. Analyst 137, 2637–2642. doi:10.1039/c2an35130g

Liu, R., Wu, D., Feng, X., Mullen, K., 2011. Bottom-up fabrication of photoluminescent graphene quantum dots with uniform morphology. J. Am. Chem. Soc. 133, 15221–15223. doi:10.1021/ja204953k

Liu, S., Zhao, N., Cheng, Z., Liu, H., 2015. Amino-functionalized green fluorescent carbon dots as surface energy transfer biosensors for hyaluronidase. Nanoscale 7, 6836–6842. doi:10.1039/C5NR00070J

Long, G.L., Winefordner, J.D., 1983. Limit of Detection A Closer Look at the IUPAC Definition. Anal. Chem. 55, 712A–724A. doi:10.1021/ac00258a724

Lu, J., Yang, J., Wang, J., Lim, A., Wang, S., Loh, K.P., 2009. One-pot synthesis of fluorescent carbon nanoribbons, nanoparticles, and graphene by the exfoliation of graphite in ionic liquids. ACS Nano 3, 2367–2375. doi:10.1021/nn900546b

Lu, J., Yeo, P.S.E., Gan, C.K., Wu, P., Loh, K.P., 2011. Transforming C_{60} molecules into graphene quantum dots. Nat Nano 6, 247–252.

Lu, W., Qin, X., Liu, S., Chang, G., Zhang, Y., Luo, Y., Asiri, A.M., Al-Youbi, A.O., Sun, X., 2012. Economical, green synthesis of fluorescent carbon nanoparticles and their use as probes for sensitive and selective detection of mercury(II) ions. Anal. Chem. 84, 5351–5357. doi:10.1021/ac3007939

Luo, Z., Lim, S., Tian, Z., Shang, J., Lai, L., MacDonald, B., Fu, C., Shen, Z., Yu, T., Lin, J., 2011. Pyridinic N doped graphene: synthesis, electronic structure and electrocatalytic property. J. Mater. Chem. 21, 8038–8044. doi:10.1039/C1JM10845J

McDonald-Wharry, J., Manley-Harris, M., Pickering, K., 2013. Carbonisation of biomass-derived chars and the thermal reduction of a graphene oxide sample studied using Raman spectroscopy. Carbon 59, 383–405. doi:http://dx.doi.org/10.1016/j.carbon.2013.03.033

Mehta, V.N., Jha, S., Basu, H., Singhal, R.K., Kailasa, S.K., 2015. One-step hydrothermal approach to fabricate carbon dots from apple juice for imaging of mycobacterium and fungal cells. Sensors Actuators B Chem. 213, 434–443. doi:http://dx.doi.org/10.1016/j.snb.2015.02.104

Mehta, V.N., Jha, S., Kailasa, S.K., 2014. One-pot green synthesis of carbon dots by using Saccharum officinarum juice for fluorescent imaging of bacteria (*Escherichia coli*) and yeast (*Saccharomyces cerevisiae*) cells. Mater. Sci. Eng. C 38, 20–27. doi:http://dx.doi.org/10.1016/j.msec.2014.01.038

Mewada, A., Pandey, S., Shinde, S., Mishra, N., Oza, G., Thakur, M., Sharon, M., Sharon, M., 2013. Green synthesis of biocompatible carbon dots using aqueous extract of *Trapa bispinosa* peel. Mater. Sci. Eng. C 33, 2914–2917. doi:http://dx.doi.org/10.1016/j.msec.2013.03.018

Na, W., Liu, X., Pang, S., Su, X., 2015. Highly sensitive detection of 2,4,6-trinitrophenol (TNP) based on lysozyme capped CdS quantum dots. RSC Adv. 5, 51428–51434. doi:10.1039/C5RA06101F

Ohno, Y., Maehashi, K., Matsumoto, K., 2010. Label-free biosensors based on aptamer-modified graphene field-effect transistors. J. Am. Chem. Soc. 132, 18012–18013. doi:10.1021/ja108127r

Pal, A., Sk, M.P., Chattopadhyay, A., 2016. Conducting Carbon Dot-Polypyrrole Nanocomposite for Sensitive Detection of Picric acid. ACS Appl. Mater. Interfaces 8, 5758–5762. doi:10.1021/acsami.5b11572

Pan, D., Zhang, J., Li, Z., Wu, M., 2010. Hydrothermal route for cutting graphene sheets into blue-luminescent graphene quantum dots. Adv. Mater. 22, 734–738. doi:10.1002/adma.200902825

Peng, H., Travas-Sejdic, J., 2009. Simple aqueous solution route to luminescent carbogenic dots from carbohydrates. Chem. Mater. 21, 5563–5565. doi:10.1021/cm901593y

Peng, J., Gao, W., Gupta, B.K., Liu, Z., Romero-Aburto, R., Ge, L., Song, L.,

Alemany, L.B., Zhan, X., Gao, G., Vithayathil, S.A., Kaipparettu, B.A., Marti, A.A., Hayashi, T., Zhu, J.-J., Ajayan, P.M., 2012. Graphene quantum dots derived from carbon fibers. Nano Lett. 12, 844–849. doi:10.1021/nl2038979

Phadke, C., Mewada, A., Dharmatti, R., Thakur, M., Pandey, S., Sharon, M., 2015. Biogenic Synthesis of Fluorescent Carbon Dots at Ambient Temperature Using Azadirachta indica (Neem) gum. J. Fluoresc. 25, 1103–1107. doi:10.1007/s10895-015-1598-x

Ponomarenko, L.A., Schedin, F., Katsnelson, M.I., Yang, R., Hill, E.W., Novoselov, K.S., Geim, A.K., 2008. Chaotic Dirac Billiard in Graphene Quantum Dots. Science (80) 320, 356–358. doi:10.1126/science.1154663

Prakash, G.K.S., Paknia, F., Kulkarni, A., Narayanan, A., Wang, F., Rasul, G., Mathew, T., Olah, G.A., 2015. Taming of superacids: PVP-triflic acid as an effective solid triflic acid equivalent for Friedel–Crafts hydroxyalkylation and acylation. J. Fluor. Chem. 171, 102–112. doi:http://dx.doi.org/10.1016/j.jfluchem.2014.08.020

Qiao, Z.-A., Wang, Y., Gao, Y., Li, H., Dai, T., Liu, Y., Huo, Q., 2010. Commercially activated carbon as the source for producing multicolor photoluminescent carbon dots by chemical oxidation. Chem. Commun. 46, 8812–8814. doi:10.1039/C0CC02724C

Qu, L., Liu, Y., Baek, J.-B., Dai, L., 2010. Nitrogen-doped graphene as efficient metal-free electrocatalyst for oxygen reduction in fuel cells. ACS Nano 4, 1321–1326. doi:10.1021/nn901850u

Ray, S.C., Saha, A., Jana, N.R., Sarkar, R., 2009. Fluorescent Carbon Nanoparticles: Synthesis, Characterization, and Bioimaging Application. J. Phys. Chem. C 113, 18546–18551. doi:10.1021/jp905912n

Roushani, M., Mavaei, M., Rajabi, H.R., 2015. Graphene quantum dots as novel and green nano-materials for the visible-light-driven photocatalytic degradation of cationic dye. J. Mol. Catal. A Chem. 409, 102–109.

doi:http://dx.doi.org/10.1016/j.molcata.2015.08.011

Sahu, S., Behera, B., Maiti, T.K., Mohapatra, S., 2012. Simple one-step synthesis of highly luminescent carbon dots from orange juice: application as excellent bio-imaging agents. Chem. Commun. 48, 8835–8837. doi:10.1039/C2CC33796G

Shang, J., Ma, L., Li, J., Ai, W., Yu, T., Gurzadyan, G.G., 2012. The Origin of Fluorescence from Graphene Oxide. Sci. Rep. 2, 792.

Shen, J., Zhu, Y., Chen, C., Yang, X., Li, C., 2011. Facile preparation and upconversion luminescence of graphene quantum dots. Chem. Commun. 47, 2580–2582. doi:10.1039/C0CC04812G

Shen, J., Zhu, Y., Yang, X., Li, C., 2012. Graphene quantum dots: emergent nanolights for bioimaging, sensors, catalysis and photovoltaic devices. Chem. Commun. 48, 3686–3699. doi:10.1039/C2CC00110A

Shi, B., Zhang, L., Lan, C., Zhao, J., Su, Y., Zhao, S., 2015. One-pot green synthesis of oxygen-rich nitrogen-doped graphene quantum dots and their potential application in pH-sensitive photoluminescence and detection of mercury(II) ions. Talanta 142, 131–139. doi:http://dx.doi.org/10.1016/j.talanta.2015.04.059

Shi, D., Yan, F., Zheng, T., Wang, Y., Zhou, X., Chen, L., 2015. P-doped carbon dots act as a nanosensor for trace 2,4,6-trinitrophenol detection and a fluorescent reagent for biological imaging. RSC Adv. 5, 98492–98499. doi:10.1039/C5RA18800H

Sun, H., Wu, L., Gao, N., Ren, J., Qu, X., 2013. Improvement of photoluminescence of graphene quantum dots with a biocompatible photochemical reduction pathway and its bioimaging application. ACS Appl. Mater. Interfaces 5, 1174–1179. doi:10.1021/am3030849

Sun, Y.-P., Zhou, B., Lin, Y., Wang, W., Fernando, K.A.S., Pathak, P., Meziani, M.J., Harruff, B.A., Wang, X., Wang, H., Luo, P.G., Yang, H., Kose, M.E., Chen, B., Veca, L.M., Xie, S.-Y., 2006. Quantum-sized carbon dots for bright and colorful photoluminescence. J. Am. Chem. Soc. 128, 7756–7757.

doi:10.1021/ja062677d

Thambiraj, S., Ravi Shankaran, D., 2016. Green synthesis of highly fluorescent carbon quantum dots from sugarcane bagasse pulp. Appl. Surf. Sci. 390, 435–443. doi:http://dx.doi.org/10.1016/j.apsusc.2016.08.106

Tripathi, K.M., Sonker, A.K., Sonkar, S.K., Sarkar, S., 2014. Pollutant soot of diesel engine exhaust transformed to carbon dots for multicoloured imaging of E. coli and sensing cholesterol. RSC Adv. 4, 30100–30107. doi:10.1039/C4RA03720K

Umrao, S., Jang, M.-H., Oh, J.-H., Kim, G., Sahoo, S., Cho, Y.-H., Srivastva, A., Oh, I.-K., 2015. Microwave bottom-up route for size-tunable and switchable photoluminescent graphene quantum dots using acetylacetone: New platform for enzyme-free detection of hydrogen peroxide. Carbon 81, 514–524. doi:http://dx.doi.org/10.1016/j.carbon.2014.09.084

Wang, F., Pang, S., Wang, L., Li, Q., 2010. One-Step Synthesis of Highly Luminescent Carbon Dots in Noncoordinating Solvents 22, 4528–4530. doi:10.1021/cm101350u

Wang, J., Wang, C.-F., Chen, S., 2012. Amphiphilic egg-derived carbon dots: rapid plasma fabrication, pyrolysis process, and multicolor printing patterns. Angew. Chem. Int. Ed. Engl. 51, 9297–9301. doi:10.1002/anie.201204381

Wang, L., Li, W., Wu, B., Li, Z., Wang, S., Liu, Y., Pan, D., Wu, M., 2016. Facile synthesis of fluorescent graphene quantum dots from coffee grounds for bioimaging and sensing. Chem. Eng. J. 300, 75–82. doi:http://dx.doi.org/10.1016/j.cej.2016.04.123

Wang, Y., Shao, Y., Matson, D.W., Li, J., Lin, Y., 2010. Nitrogen-doped graphene and its application in electrochemical biosensing. ACS Nano 4, 1790–1798. doi:10.1021/nn100315s

Wee, S.S., Ng, Y.H., Ng, S.M., 2013. Synthesis of fluorescent carbon dots via simple acid hydrolysis of bovine serum albumin and its potential as sensitive sensing probe for lead (II) ions. Talanta 116, 71–76.

doi:http://dx.doi.org/10.1016/j.talanta.2013.04.081

Weng, C.-I., Chang, H.-T., Lin, C.-H., Shen, Y.-W., Unnikrishnan, B., Li, Y.-J., Huang, C.-C., 2015. One-step synthesis of biofunctional carbon quantum dots for bacterial labeling. Biosens. Bioelectron. 68, 1–6. doi:http://dx.doi.org/10.1016/j.bios.2014.12.028

Yan, X., Cui, X., Li, L.-S., 2010. Synthesis of large, stable colloidal graphene quantum dots with tunable size. J. Am. Chem. Soc. 132, 5944–5945. doi:10.1021/ja1009376

Yan, X., Li, B., Li, L., 2013. Colloidal graphene quantum dots with well-defined structures. Acc. Chem. Res. 46, 2254–2262. doi:10.1021/ar300137p

Yang, X., Zhuo, Y., Zhu, S., Luo, Y., Feng, Y., Dou, Y., 2014. Novel and green synthesis of high-fluorescent carbon dots originated from honey for sensing and imaging. Biosens. Bioelectron. 60, 292–298. doi:10.1016/j.bios.2014.04.046

Yang, Y., Cui, J., Zheng, M., Hu, C., Tan, S., Xiao, Y., Yang, Q., Liu, Y., 2012. One-step synthesis of amino-functionalized fluorescent carbon nanoparticles by hydrothermal carbonization of chitosan. Chem. Commun. 48, 380–382. doi:10.1039/C1CC15678K

Yu, J.-G., Yu, L.-Y., Yang, H., Liu, Q., Chen, X.-H., Jiang, X.-Y., Chen, X.-Q., Jiao, F.-P., 2015. Graphene nanosheets as novel adsorbents in adsorption, preconcentration and removal of gases, organic compounds and metal ions. Sci. Total Environ. 502, 70–79. doi:http://dx.doi.org/10.1016/j.scitotenv.2014.08.077

Yu, J., Song, N., Zhang, Y.-K., Zhong, S.-X., Wang, A.-J., Chen, J., 2015. Green preparation of carbon dots by *Jinhua bergamot* for sensitive and selective fluorescent detection of Hg^{2+} and Fe^{3+}. Sensors Actuators B Chem. 214, 29–35. doi:http://dx.doi.org/10.1016/j.snb.2015.03.006

Yuan, H., Yu, J., Feng, S., Gong, Y., 2016. Highly photoluminescent pH-independent nitrogen-doped carbon dots for sensitive and selective sensing of p-nitrophenol. RSC Adv. 6, 15192–15200. doi:10.1039/C5RA26870B

Yuan, M., Zhong, R., Gao, H., Li, W., Yun, X., Liu, J., Zhao, X., Zhao, G., Zhang, F., 2015. One-step, green, and economic synthesis of water-soluble photoluminescent carbon dots by hydrothermal treatment of wheat straw, and their bio-applications in labeling, imaging, and sensing. Appl. Surf. Sci. 355, 1136–1144. doi:http://dx.doi.org/10.1016/j.apsusc.2015.07.095

Zhai, X., Zhang, P., Liu, C., Bai, T., Li, W., Dai, L., Liu, W., 2012. Highly luminescent carbon nanodots by microwave-assisted pyrolysis. Chem. Commun. 48, 7955–7957. doi:10.1039/C2CC33869F

Zhang, M., Bai, L., Shang, W., Xie, W., Ma, H., Fu, Y., Fang, D., Sun, H., Fan, L., Han, M., Liu, C., Yang, S., 2012. Facile synthesis of water-soluble, highly fluorescent graphene quantum dots as a robust biological label for stem cells. J. Mater. Chem. 22, 7461–7467. doi:10.1039/C2JM16835A

Zhang, R., Chen, W., 2014. Nitrogen-doped carbon quantum dots: facile synthesis and application as a "turn-off" fluorescent probe for detection of Hg^{2+} ions. Biosens. Bioelectron. 55, 83–90. doi:10.1016/j.bios.2013.11.074

Zhang, Z., Zhang, J., Chen, N., Qu, L., 2012. Graphene quantum dots: an emerging material for energy-related applications and beyond. Energy Environ. Sci. 5, 8869–8890. doi:10.1039/C2EE22982J

Zheng, H., Wang, Q., Long, Y., Zhang, H., Huang, X., Zhu, R., 2011. Enhancing the luminescence of carbon dots with a reduction pathway. Chem. Commun. 47, 10650–10652. doi:10.1039/C1CC14741B

Zheng, L., Chi, Y., Dong, Y., Lin, J., Wang, B., 2009. Electrochemiluminescence of water-soluble carbon nanocrystals released electrochemically from graphite. J. Am. Chem. Soc. 131, 4564–4565. doi:10.1021/ja809073f

Zhou, J., Booker, C., Li, R., Zhou, X., Sham, T.-K., Sun, X., Ding, Z., 2007. An electrochemical avenue to blue luminescent nanocrystals from multiwalled carbon nanotubes (MWCNTs). J. Am. Chem. Soc. 129, 744–745. doi:10.1021/ja0669070

Zhou, Y., Qu, Z., Zeng, Y., Zhou, T., Shi, G., 2014. A novel composite of graphene quantum dots and molecularly imprinted polymer for fluorescent detection of paranitrophenol. Biosens. Bioelectron. 52, 317–323. doi:http://dx.doi.org/10.1016/j.bios.2013.09.022

Zhu, B., Sun, S., Wang, Y., Deng, S., Qian, G., Wang, M., Hu, A., 2013. Preparation of carbon nanodots from single chain polymeric nanoparticles and theoretical investigation of the photoluminescence mechanism. J. Mater. Chem. C 1, 580–586. doi:10.1039/C2TC00140C

Zhu, H., Wang, X., Li, Y., Wang, Z., Yang, F., Yang, X., 2009. Microwave synthesis of fluorescent carbon nanoparticles with electrochemiluminescence properties. Chem. Commun. 5118–5120. doi:10.1039/B907612C

Zhu, S., Zhang, J., Liu, X., Li, B., Wang, X., Tang, S., Meng, Q., Li, Y., Shi, C., Hu, R., Yang, B., 2012. Graphene quantum dots with controllable surface oxidation, tunable fluorescence and up-conversion emission. RSC Adv. 2, 2717–2720. doi:10.1039/C2RA20182H

Zhu, S., Zhang, J., Qiao, C., Tang, S., Li, Y., Yuan, W., Li, B., Tian, L., Liu, F., Hu, R., Gao, H., Wei, H., Zhang, H., Sun, H., Yang, B., 2011. Strongly green-photoluminescent graphene quantum dots for bioimaging applications. Chem. Commun. 47, 6858–6860. doi:10.1039/C1CC11122A

Zhuo, S., Shao, M., Lee, S.-T., 2012. Upconversion and downconversion fluorescent graphene quantum dots: ultrasonic preparation and photocatalysis. ACS Nano 6, 1059–1064. doi:10.1021/nn2040395

Zong, J., Zhu, Y., Yang, X., Shen, J., Li, C., 2011. Synthesis of photoluminescent carbogenic dots using mesoporous silica spheres as nanoreactors. Chem. Commun. 47, 764–766. doi:10.1039/C0CC03092A